https://doi.org/10.1093/plphys/kiac547 PLANT PHYSIOLOGY 2023: 191: 904–924

Plant Physiology®

Research Article

A viral movement protein co-opts endoplasmic reticulum luminal-binding protein and calreticulin to promote intracellular movement

Ying-Wen Huang [1,2], Chu-I Sun,[1] Chung-Chi Hu [1,2], Ching-Hsiu Tsai [1,2], Menghsiao Meng [1], Na-Sheng Lin [3], Savithramma P. Dinesh-Kumar [4] and Yau-Heiu Hsu [1,2,*]

1 Graduate Institute of Biotechnology, National Chung Hisng University, Taichung 40227, Taiwan
2 Advanced Plant Biotechnology Center, National Chung Hsing University, Taichung 40227, Taiwan
3 Institute of Plant and Microbial Biology, Academia Sinica, Taipei 11529, Taiwan
4 Department of Plant Biology and The Genome Center, College of Biological Sciences, University of California, Davis, Davis, California 95616, USA

*Author for correspondence: yhhsu@nchu.edu.tw
The author responsible for distribution of materials integral to the findings presented in this article in accordance with the policy described in the Instructions for Authors (https://academic.oup.com/plphys/pages/General-Instructions) is Yau-Heiu Hsu (yhhsu@nchu.edu.tw).

Abstract

Intracellular movement is an important step for the initial spread of virus in plants during infection. This process requires virus-encoded movement proteins (MPs) and their interaction with host factors. Despite the large number of known host factors involved in the movement of different viruses, little is known about host proteins that interact with one of the MPs encoded by potexviruses, the triple-gene-block protein 3 (TGBp3). The main obstacle lies in the relatively low expression level of potexviral TGBp3 in hosts and the weak or transient nature of interactions. Here, we used TurboID-based proximity labeling to identify the network of proteins directly or indirectly interacting with the TGBp3 of a potexvirus, *Bamboo mosaic virus* (BaMV). Endoplasmic reticulum (ER) luminal-binding protein 4 and calreticulin 3 of *Nicotiana benthamiana* (NbBiP4 and NbCRT3, respectively) associated with the functional TGBp3-containing BaMV movement complexes, but not the movement-defective mutant, TGBp3M. Fluorescent microscopy revealed that TGBp3 colocalizes with NbBiP4 or NbCRT3 and the complexes move together along ER networks to cell periphery in *N. benthamiana*. Loss- and gain-of-function experiments revealed that NbBiP4 or NbCRT3 is required for the efficient spread and accumulation of BaMV in infected leaves. In addition, overexpression of *NbBiP4* or *NbCRT3* enhanced the targeting of BaMV TGBp1 to plasmodesmata (PD), indicating that NbBiP4 and NbCRT3 interact with TGBp3 to promote the intracellular transport of virion cargo to PD that facilitates virus cell-to-cell movement. Our findings revealed additional roles for NbBiP4 and NbCRT3 in BaMV intracellular movement through ER networks or ER-derived vesicles to PD, which enhances the spread of BaMV in *N. benthamiana*.

Introduction

To establish systemic invasions in hosts, plant viruses have developed various functions for critical steps in their infection cycle: replication at the initial infected cells, intracellular spreading to cell peripheries, local movement to non-infected adjacent cells, and systemic movement to other organs, and eventually invading the whole plant (Nelson and Citovsky, 2005). For functions involved in movement, plant viruses have evolved various types of proteins, termed movement proteins (MPs), to facilitate the intra and intercellular spreading of plant viruses throughout the host (Dorokhov et al., 2020). In addition, a large number of host factors and pathways (including factors in the endomembrane systems, cytoskeletal network, and secretory pathways) have been exploited by plant viruses to accomplish the tasks for movement (Kumar and Dasgupta, 2021). The comprehensive understanding of the interactions between viral MPs and host factors is important for us to reveal the details of viral infection cycles

Received September 28, 2022. Accepted November 3, 2022. Advance access publication December 3, 2022

which also provide further insights into the mechanisms of material transportations in plants (Wang, 2015; Pitzalis and Heinlein, 2018).

In contrast to animal systems, the symplasts of neighboring plant cells are interconnected through plasmodesmata (PD), consisting of plasma membranes, endomembrane, microtubule systems, and related proteins, forming channels passing through the cell wall for transportation of proteins, nucleic acids, chemicals, etc., between neighboring cells to maintain homeostasis and deliver important messages required for cell growth (Roberts and Oparka, 2003; Lucas et al., 2009; Kumar and Dasgupta, 2021). Nearly all plant viruses encode one or multiple MPs, which help the virus transport between cells through PD in the form of ribonucleoprotein (RNP) complexes, virus particles (virion), or virus replication complexes (VRCs; Kawakami et al., 2004; Lucas, 2006). Transport through PD is tightly regulated and restricted by the size exclusion limits (SELs) of different PD (Ueki and Citovsky, 2011). To overcome the physical barriers posed by cell walls and PD, different plant viruses employ specific types of MPs and adopt various strategies for successful spreading (Navarro et al., 2019; Kumar and Dasgupta, 2021). For viruses in the family *Alphaflexiviridae* (including the genus *Potexvirus*), a set of three viral proteins, termed triple-gene-block proteins (TGBps), serve as the MPs in the infection cycles.

The functions and characteristics of the three TGB proteins of potexviruses in viral movement have been well documented (Morozov and Solovyev, 2003; Verchout-Lubicz et al., 2010; Solovyev et al., 2012). TGBp1 forms inclusion bodies in the cytoplasm and nucleus (Chang et al., 1997; Samuels et al., 2007) with an RNA binding and ATPase activity (Wung et al., 1999; Hsu et al., 2004). In addition, TGBp1 exhibits helicase activity (Kalinina et al., 2002), which can increase the SEL of PD, helping the virus complexes pass through PD (Angell et al., 1996; Howard et al., 2004). In the initial virus-infected cells, TGBp1 can promote the translation of viral nucleic acid to produce replication enzymes for initiation of a new infection cycle (Atabekov et al., 2000). TGBp2 protein has two transmembrane domains and is an integral membrane protein of endoplasmic reticulum (ER) and ER-derived vesicles (Ju et al., 2005; Hsu et al., 2008). The TGBp2-containing ER vesicles can align on the actin network during virus infection (Ju et al., 2005). Deletion or substitution of the highly conserved amino acid sequence in the TGBp2 central loop, which is located in the ER lumen, inhibits vesicle formation and viral cell-to-cell movement (Ju et al., 2007). Two C-terminal conserved cysteine (Cys) residues of *Bamboo mosaic virus* (BaMV) TGBp2 are important for targeting TGBp1 to PD and hence are critical for cell-to-cell movement of BaMV (Tseng et al., 2009; Ho et al., 2017). TGBp3 is an ER integral membrane protein with single transmembrane domain (Lee et al., 2010); the C-terminus is hydrophilic and is exposed to the cytoplasm (Chou et al., 2013). The sorting signal in the C-terminus of TGBp3 is highly conserved in the genus *Potexvirus* and promotes targeting of TGBp2 to the cortical ER at the cell periphery (Lee et al., 2010; Wu et al., 2011). In addition, two conserved Cys residues in the C-terminus of TGBp3 play a key role in BaMV cell-to-cell movement by enhancing the TGBp2- and TGBp3-dependent PD localization of TGBp1 (Chou et al., 2013). Our previous results suggested that the cell-to-cell movement of BaMV requires an association of the virion cargo with the TGBp2- and TGBp3-based membrane complexes and recruitment of TGBp1, with TGBp3 playing a key role in carrying the entire virus movement complexes along the ER network or actin filament to PD. Subsequently, the SEL of PD is increased via TGBp1 so that the virion cargo can pass through PD to the adjacent uninfected cells (Chou et al., 2013; Liou et al., 2015).

In addition to viral proteins, viruses in the family *Alphaflexiviridae* also exploit host proteins or subcellular structures to facilitate the movement functions. Some of these host factors have been demonstrated to interact with the TGBps of alphaflexiviruses. TGBp1 is known to reorganize host protein actin and endomembrane, forming the protective structure, X-body, for *Potato virus X* (PVX) replication, assembly, and movement (Tilsner et al., 2012). The nucleolar proteins fibrillarin and coilin have been shown to interact with TGBp1 of hordeivirus (Semashko et al., 2012a, 2012b) or potexvirus (Chang et al., 2016), taking part in the formation of viral and subviral RNPs involved in long-distance movement (Solovyev et al., 2012; Chang et al., 2016). The interaction of TGBp1 with a host membrane raft protein, StRemorin1.3 may hamper the movement of PVX (Perraki et al., 2014), whereas the interaction with a casein kinase 2-like protein may result in the phosphorylation of TGBp1 and promote viral movement (Módena et al., 2008; Hu et al., 2015). For TGBp2-interacting host proteins, it has been demonstrated that β-1,3-glucanase-associated host factor TIP1 (TGB12K-interacting protein 1) may interact with TGBp2 and β-1,3-glucanase, thereby decreasing the callose accumulation in PD to facilitate viral intercellular trafficking (Fridborg et al., 2003; Reagan and Burch-Smith, 2020). In addition, a serine/threonine kinase-like protein of *Nicotiana benthamiana* (NbSTKL) and a Rab GTPase activation protein 1 (NbRabGAP1) have been shown to contribute to the intracellular movement of BaMV (Cheng et al., 2013; Huang et al., 2013). For TGBp3, it has been shown that PVX TGBp3 may induce unfolded protein response and SKP1-dependent programmed cell death (Ye et al., 2013). Despite the rich body of information regarding the host proteins interacting with TGBp1 and/or TGBp2 for the movement of viruses in the family Alphaflexiviridae, no host proteins have been demonstrated to interact, either directly or non-directly, with TGBp3. The main obstacles possibly lies in the relatively low abundance of TGBp3, when compared with TGBp1 and TGBp2, and the weak and transient characteristics of the interactions anticipated between proteins involved in movement functions. To explore the interaction network involving TGBp3 for viral movement, we have focused on an extensively studied potexvirus, BaMV.

BaMV belongs to the genus *Potexvirus* in family *Alphaflexiviridae* (Hsu et al., 2018). The genome of BaMV is a single-stranded RNA molecule. It encodes five genes (Lin et al., 1994; Yang et al., 1997). The first gene produces an enzyme that is responsible for building the viral replication factories and copying the viral RNA (vRNA; Meng and Lee, 2017). The overlapping second to fourth genes encode the TGBps required for viral movement, characteristic to viruses in the genus *Potexvirus* (Morozov and Solovyev, 2003; Chou et al., 2013). BaMV TGBp1 has also been shown to be an RNA silencing suppressor in BaMV infection (Huang et al., 2019). The last gene encodes a CP for virion assembly, movement, and symptom development (Lan et al., 2010; Hung et al., 2014; DiMaio et al., 2015).

In this study, we used TurboID-based proximity labeling (PL) approach to explore the interaction networks of BaMV TGBp3 in planta during BaMV infection on *N. benthamiana*. TurboID is a biotin ligase that catalyzes PL of proteins within a radius of a few nanometers and has emerged as an innovative technique to study the interactions of proteins, including those with weak, transient, or indirect associations, within plant cells (Branon et al., 2018; Zhang et al., 2019; Zhang et al., 2020). Among the host factors identified within the proximity of BaMV TGBp3, two ER-resident proteins, luminal-binding protein 4 and calreticulin 3 of *N. benthamiana* (designated NbBiP4 and NbCRT3, respectively), were further analyzed for their possible roles in the movement of BaMV. The results revealed that NbBiP4 and NbCRT3 only interact with the movement-competent BaMV TGBp3, but not the movement-defective mutant TGBp3M, and that these proteins positively regulate the cell-to-cell movement of specific viruses, including BaMV. The possible role of these ER-resident proteins in viral movement is further discussed. These results reveal additional function of ER-resident proteins, NbBiP4 and NbCRT3, in facilitating the movement of specific viruses, and provide further insights into the transportation of materials as large as VRCs within and between plant cells.

Results

Expression of TGBp3-TurboID efficiently biotinylates host proteins

Since BaMV TGBp3 is critical for transporting the movement complexes containing TGBp1, TGBp2, and TGBp3 along the ER network (Wu et al., 2011; Chou et al., 2013), we used TGBp3 to identify host factors involved in the transport of BaMV movement complexes. The cDNA fragments of BaMV TGBp3 and TGBp2p3 were cloned into the upstream region of TurboID (TbID) expression cassette, generating the plasmids p35S::TGBp3-TbID and p35S::TGBp2p3-TbID, respectively (Figure 1A). With the expression of p35S::TGBp2p3-TbID, TGBp2 and TGBp3-TbID tagged with triple human influenza hemagglutinin epitope (TGBp3-TbID-3XHA) proteins were translated in the same cell (Figure 1A, right). In contrast, for p35S::TGBp3-TbID, only TGBp3-TbID-3XHA were expressed (Figure 1A, right). As a control, we generated TurboID fused to the C-terminal of TGBp3 with sorting signal mutation (I33A and I35A, TGBp3M), which would not be transported to the cortical ER (Wu et al., 2011). In order to validate the functionalities of different TGBp3 constructs with TbID fusion tag in BaMV cell-to-cell movement, the following complementation assays were performed. A TGBp3-defective BaMV infectious clone, pCBGp3ATGm, was constructed by substitution of the initiation codon, ATG, of TGBp3 gene to CTG that would disrupt the translation initiation of TGBp3 while retaining the codon of TGBp2. The infectious clones carry green fluorescent protein (GFP) gene expressed from a duplicated CP subgenomic promoter (Lin et al., 2004), allowing for visualization of the BaMV-infected cells via fluorescence (Supplemental Figure 1A). The inoculation assay revealed that accumulation levels of genomic RNA, subgenomic RNAs, and CP of BaMV in protoplasts inoculated with infectious constructs of wild-type BaMV (pCBGp3HA) or TGBp3-defected BaMV (pCBGp3ATGm) were similar, indicating that TGBp3-defective BaMV retained a wild-type replication activity (Supplemental Figure 1B). The result of Western blot analyses showed the corresponding expression of TGBp3HA could be detected in pCBGp3HA- but not in pCBGp3ATGm-inoculated cells (Supplemental Figure 1B, right panel). In the trans-complementation assays, the TbID alone (control) or TGBp3 fusions were transiently expressed in *N. benthamiana* for one day and then the virions of wild-type BaMV (BGp3HA) or TGBp3-defective BaMV (BGp3ATGm) were inoculated into the leaves. Following the cultivation of inoculated plants for an additional three days, the leaves were examined with fluorescence microscopy. The result revealed that clusters of green fluorescent cells could be observed in leaves inoculated with BGp3HA plus expression of TbID, but not in the leaves inoculated with BGp3ATGm, as expected due to defects in cell-to-cell movement (Supplemental Figure 1C, i and ii). When trans-complemented with TGBp3-T7, TGBp3-TbID, or TGBp2p3-TbID in infection of BGp3ATGm, the green fluorescent (GF) clusters were observed (Supplemental Figure 1D, iii, iv, and vi). However, in the leaves complemented with TGBp3M-TbID or TGBp2p3M-TbID, only restricted GF movements from the initial infection foci (Supplemental Figure 1C, v and vii) were observed. Western blot analysis with corresponding antibodies confirmed the expression of these proteins (Supplemental Figure 1D). These data showed TGBp3-TbID fusion can complement the ability of BGp3ATGm to move from cell to cell, thus demonstrating the functionality of TbID-fused TGBp3 in BaMV cell-to-cell movement.

To assess if TGBp3-TbID fusion could promote cis-biotinylation and trans-biotinylation of host proteins, agrobacterium harboring TGBp3-TbID, TGBp2p3-TbID, TGBp3M-TbID, and TGBp2p3M-TbID were co-infiltrated with BaMV into *N. benthamiana* plants. At 2 days post-agroinfiltration (dpai), 200 μM biotin was infiltrated into the leaves and incubated for an additional 8 h. Immunoblot analysis, with horseradish peroxidase (HRP)-conjugated streptavidin

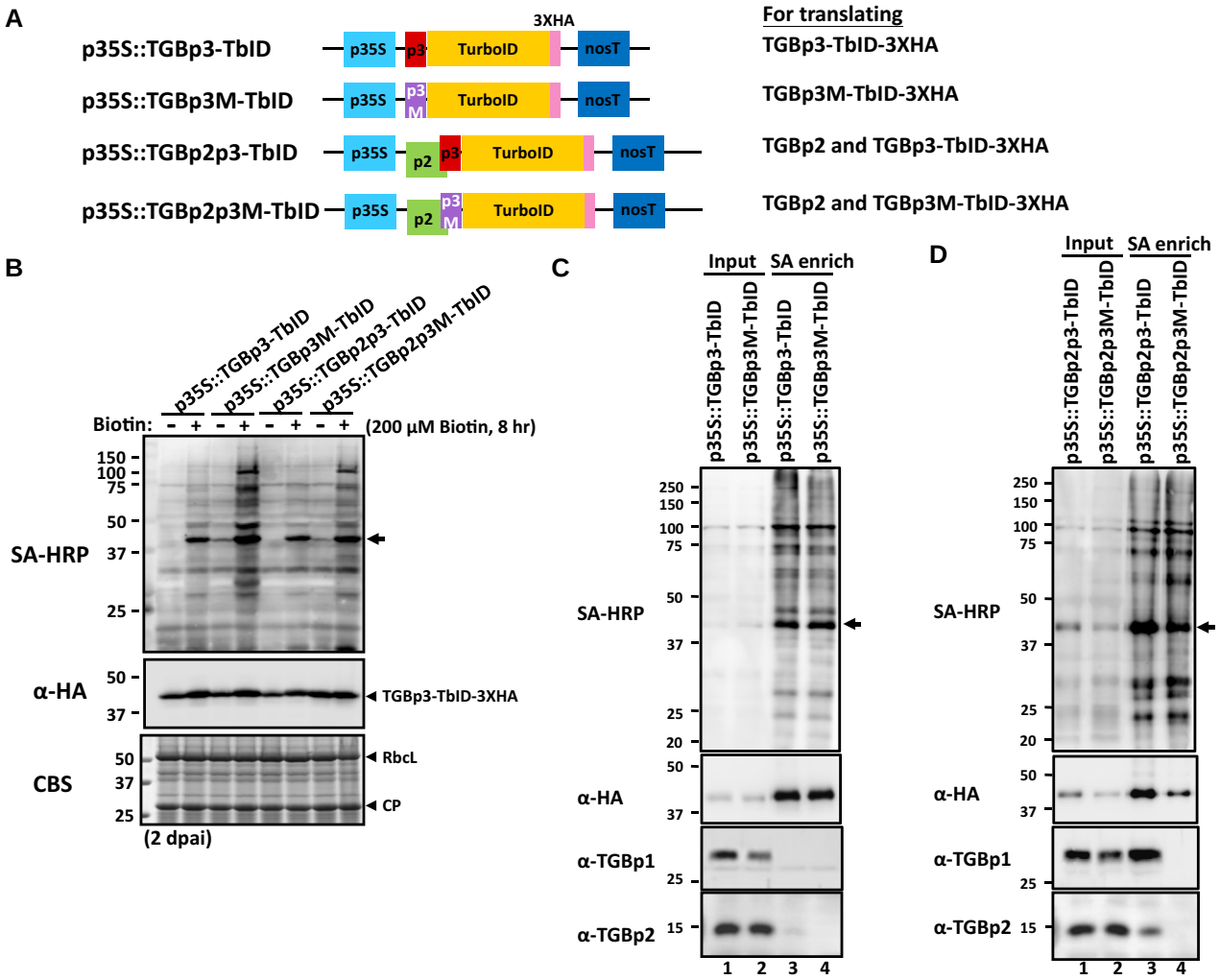

Figure 1 TurboID-based PL of BaMV TGBp3 interactors in *N. benthamiana*. A, Schematic representation of the constructs used for identifying proximal and interacting proteins of BaMV TGBp3 or TGBp3M (I33,35A mutation). Gene expression was under the control of the 35S promoter (p35S) and nopaline synthase terminator (nosT). The translated proteins from each mRNA are indicated on the right. p2, TGBp2; p3, TGBp3; p3M, TGBp3M; HA, hemagglutinin. B, Biotin ligase activity of TGBp3-TbID or TGBp3M-TbID in BaMV-infected *N. benthamiana*. *N. benthamiana* leaves were agroinfiltrated with *Agrobacterium* containing p35S::TGBp3-TbID, p35S::TGBp3M-TbID, p35S::TGBp2p3-TbID, or p35S::TGBp2p3M-TbID. After 2 days post-agroinfiltration (dpai), buffer with (+) or without (−) 200 µM biotin was infiltrated into the infiltrated leaves and incubated for an additional 8 h. Streptavidin-HRP (SA-HRP) and anti-HA antibodies were used for detecting biotinylated proteins (top panel) and TGBp3-TbID-3XHA variants (middle panel), respectively. Coomassie blue staining (CBS) served as a loading control (bottom panel). The arrow on the right indicates the position of self-biotinylated TGBp3-TbID or TGBp3M-TbID. Prestained protein markers with molecular mass (in kDa) are shown on the left. CP, BaMV coat protein; RbcL, RuBisCO large subunit. C and D, Detection of total biotinylated proteins before (Input) and after, respectively, enrichment with streptavidin-coupled beads (SA enrich). Anti-TGBp1 antibody was used for detecting BaMV TGBp1 in input and SA-enriched fraction.

(SA-HRP) revealed that all TurboID fusion proteins had biotinylation activity (Figure 1B, upper panel). Immunoblot assay with anti-hemagglutinin (HA) antibody revealed no discernible differences in the expression of TGBp3 among different constructs (Figure 1B, middle panel). The biotinylated proteins were then enriched from the total extracted proteins by using SA-coupled magnetic beads. The enriched biotinylated proteins were confirmed by Western blot analysis with SA-HRP or anti-HA antibody (Figure 1, C and D). To determine whether the SA-enriched TGBp3-associated complexes contained other two BaMV MPs, TGBp1 and TGBp2, immunoblot assays with anti-TGBp1 or anti-TGBp2 antibody were performed. The result showed that only TGBp2p3-TbID could co-precipitate TGBp1 and TGBp2 but not TGBp2p3M-TbID (Figure 1D, lower panel). These results suggested that TGBp2p3M interferes with the interaction network of BaMV movement complexes, so TGBp3M may serve as an appropriate control in PL experiments to differentiate the host factors within the BaMV movement complexes. Note that TGBp2p3-TbID co-precipitated more TGBp2 and TGBp1

than did TGBp3-TbID alone (Figure 1, compare lanes 3 in Figure 1, C and D), indicating that the co-translation of TGBp2 and TGBp3 may enhance the formation of intact movement complexes. Therefore, we used TGBp2p3-TbID and TGBp2p3M-TbID to analyze the protein interaction network of BaMV movement complexes in the following experiments.

Identification of interactors of BaMV TGBp3 MP

To identify TGBp3 interactors, the biotinylated proteins were SA-enriched and subjected to LC/MS-MS analysis. A total of 52 and 49 *N. benthamiana* proteins were identified in TGBp2p3-TbID- and TGBp2p3M-TbID-agroinfiltrated plants, respectively (Figure 2A and Supplemental Table 1). After subtracting the biotinylated proteins from TGBp3M-TbID, 28 unique proteins were identified in the TGBp3-TbID sample. The proteins biotinylated by TGBp3-TbID included BaMV proteins, host factors that were previously identified in the BaMV VRC or involved in BaMV cell-to-cell movement, ER proteins, cytoskeleton proteins, proteins involved in vesicle formation, metabolic enzymes, and others (Figure 2B). Since TGBp2 and TGBp3 MPs are ER integral membrane proteins, the ER luminal-binding protein (NbBiP4) and calreticulin (NbCRT3), which were among the top four of Mascot score list of the interacting host proteins (Supplemental Table 1A), were selected for further analysis based on the hypothesis that BaMV TGBp3 might co-opt NbBiP4 or NbCRT3 for viral movement along the ER network or ER-derived vesicles.

BaMV TGBp3 interacts with NbBiP4 and NbCRT3

We first tested whether BaMV TGBp3 associates with NbBiP4 or NbCRT3 by using GFP pull-down assay. NbBiP4-GFP, NbCRT3-GFP, or GFP (control) was co-expressed with TGBp3-TbID with transfection of pKBRepHA21, a BaMV infectious clone expressing HA-tagged replicase (Huang et al., 2017b). The result of GFP pull-down assay showed that NbBiP4-GFP or NbCRT3-GFP, but not GFP alone, could co-precipitate TGBp3-TbID-3XHA (Figure 3A, right panel). In addition, BaMV-CP, TGBp1, and replicase-HA were detected in the NbBiP4 or NbCRT3 pull-down complexes (Figure 3A, right panel). Furthermore, in vivo bimolecular fluorescence complementation (BiFC) assays (Citovsky et al., 2006) were performed to determine whether BaMV TGBp3 interacts with NbBiP4 or NbCRT3 in plants. As a positive control, NbBiP4-nEYFP and NbCRT3-cEYFP were transiently co-expressed in *N. benthamiana*, and intense fluorescence was observed in epidermal cells at 3 dpai (Figure 3B), due to the interaction between NbBiP4 and NbCRT3, which were in accordance with the previous report (Crofts et al., 1998). Bright yellow fluorescence was also observed when *N. benthamiana* leaves were co-infiltrated with nEYFP-TGBp3 and NbBiP4-cEYFP, or nEYFP-TGBp3 and NbCRT3-cEYFP (Figure 3B), suggesting that BaMV TGBp3 and NbBiP4 or NbCRT3 can indeed interact with each other in *N. benthamiana* cells. In contrast, no fluorescence signals were observed in *N. benthamiana* cells co-infiltrated with nEYFP and NbBiP4-cEYFP, nEYFP and NbCRT3-cEYFP, or nEYFP-TGBp3 and cEYFP, which were used as negative controls (Figure 3B). These observations demonstrate that NbBiP4 and NbCRT3 may interact with BaMV TGBp3, which might be involved in transporting the entire BaMV movement complexes in the form of RNP, virion, or even the VRC.

TGBp3 colocalizes and moves with NbBiP4 and NbCRT3 along the ER network

To investigate the colocalization of BaMV TGBp3 with NbBiP4 or NbCRT3 in vivo, we first examined their subcellular location in epidermal cells of *N. benthamiana*. The result revealed that GFP-TGBp3, NbBiP4-GFP, and NbCRT3-GFP were localized in the ER, which was visualized with ER-rk, an ER marker with mCherry fluorescent protein fusion (Nelson et al., 2007; Supplemental Figure 2). GFP-TGBp3 was localized as punctate structures, which is consistent with a previous report demonstrating that BaMV TGBp3 recruits TGBp2 to the peripheral bodies near the cell cortex in plants (Lee et al., 2010; Wu et al., 2011). Subsequently, a plasmid for the expression of orange fluorescent protein (OFP)-tagged TGBp3 (OFP-TGBp3) was constructed to determine whether TGBp3 colocalizes with NbBiP4-GFP or NbCRT3-GFP. Consistent with the localization pattern of GFP-TGBp3 in epidermal cells of *N. benthamiana* (Supplemental Figure 2), OFP-TGBp3 localized as punctate structures, but developed to a large complex after BaMV infection for 2 days (Figure 4A). These large complexes of OFP-TGBp3 were colocalized with NbBiP4-GFP and NbCRT3-GFP (Figure 4B). Time lapse imaging showed that these complexes move around within the cell dynamically (Supplemental Movies 1, A–D). The movement of vesicle-like structures with the colocalization of OFP-TGBp3 and NbCRT3-GFP were also observed in Supplemental Movie 1D. At 3 dpai, OFP-TGBp3 colocalized with NbBiP4-GFP or NbCRT3-GFP at the cortical ER with punctate structures (Figure 4C). The punctate bodies of OFP-TGBp3 were observed to move along the ER at the cell periphery with slower speed than did the complexes at 2 dpai (Supplemental Movies 1, E–H). Combined with the data from pull-down assays and movies, these results indicated that NbBiP4 or NbCRT3 may facilitate the mobilization of BaMV TGBp3 or the entire movement complexes within the cell and eventually to the cell periphery, possibly aiming to spread to the neighboring cells.

Knockdown of NbBiP4 or NbCRT3 expression suppresses BaMV accumulation

To characterize the role of NbBiP4 or NbCRT3 in BaMV infection, we used *Tobacco rattle virus* (TRV)-based virus-induced gene silencing (VIGS) approach to knockdown the expression of *NbBiP4* or *NbCRT3*. Plants infiltrated with the *Luciferase* (Luc)-silencing construct were used as the negative control. Reverse transcription quantitative PCR (RT-qPCR) analysis demonstrated that the transcription of *NbBiP4* or *NbCRT3*

A

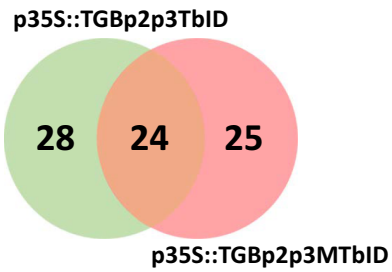

B List of proteins that are proximal to TGBp3-TbID

Protein name	Accession	Score	GO-Biological process
Viral protein (BaMV)			
Replicase	AAD48519.1	1078	
TGBp1	BAA05035.1	1130	
TGBp2	AAB70564.1	1118	
CP	AAB70566.1	4994	
HF in BaMV VRC			
GAPDH	BAP91041.1	1769	Glucose metabolic process
PGK	ADR71054.1	1615	Glycolytic process
Hsp70	ARH56399.1	1276	Protein folding
Hsp90	AAR12194.1	615	Protein folding
Putative methyltransferase	ACA66248.1	1126	Methylation
eEF1α	AAP04393.1	930	Translational elongation
Plastid carbonic anhydrase	ASW15992.1	548	Carbon utilization
HF involved in BaMV cell-to-cell movement			
Serine/threonine-protein kinase HT1	APY20265.1	19	Protein phosphorylation
ER protein			
ER luminal-binding protein 4 (BiP4)	ACK55195.1	2297	Protein folding
Calreticulin 3 (CRT3)	BBF45633.1	1588	Protein folding
Cytoskeleton protein			
Actin	AFD62804.1	611	Cell motility
Alpha-tubulin	ALH22047.1	394	Microtubule-based process
Vesicle formation			
ADP-ribosylation factor 1	ABF74733.1	154	GTP binding
RabE1	AFI98561.1	122	Vesicle docking
Nucleus protein			
Nuclear pore complex protein gp210a	BAO49720.1	757	ND
Nuclear pore complex protein gp210b	BAO49721.1	406	ND
Chloroplast protein			
RbcS	CUA55116.1	463	Photorespiration
Geranylgeranyl reductase	CAE47826.1	422	Photosynthesis
Metabolic enzyme			
S-adenosyl homocysteine hydrolase	AFK08605.1	966	S-adenosylmethionine cycle
S-adenosyl methionine synthetase	BAR72289.1	311	S-adenosylmethionine cycle
Glycolate oxidase	ADM26718.1	377	Photorespiration
Phospholipase D beta	BAS29956.1	238	Lipid catabolic process

Figure 2 BaMV TGBp3-interacting proteins. A, Schematic Venn diagram of biotinylated proteins identified by LC/MS-MS from BaMV-infected *N. benthamiana* plants with expression of p35S::TGBp2p3-TbID (left) and p35S::TGBp2p3M-TbID (right). B, List of viral proteins and selected *N. benthamiana* proteins that are proximal to TGBp3-TbID. The proteins identified uniquely from TGBp3-TbID_PL or overlapped with TGBp3M-TbID_PL are indicated in green and orange, respectively.

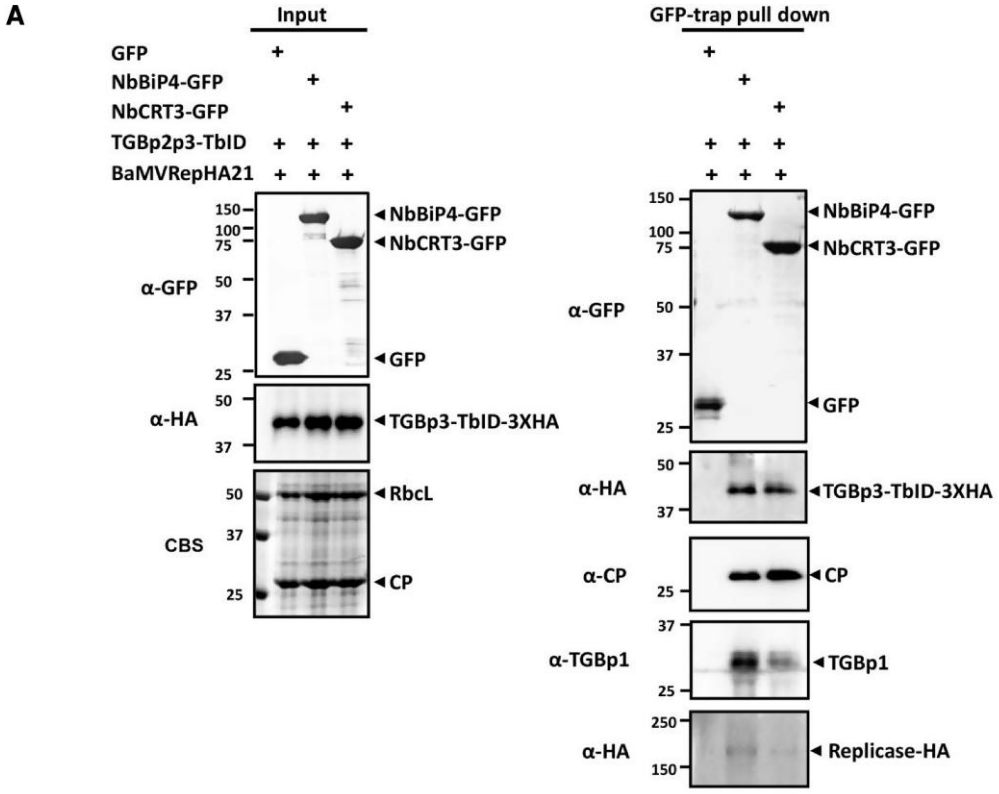

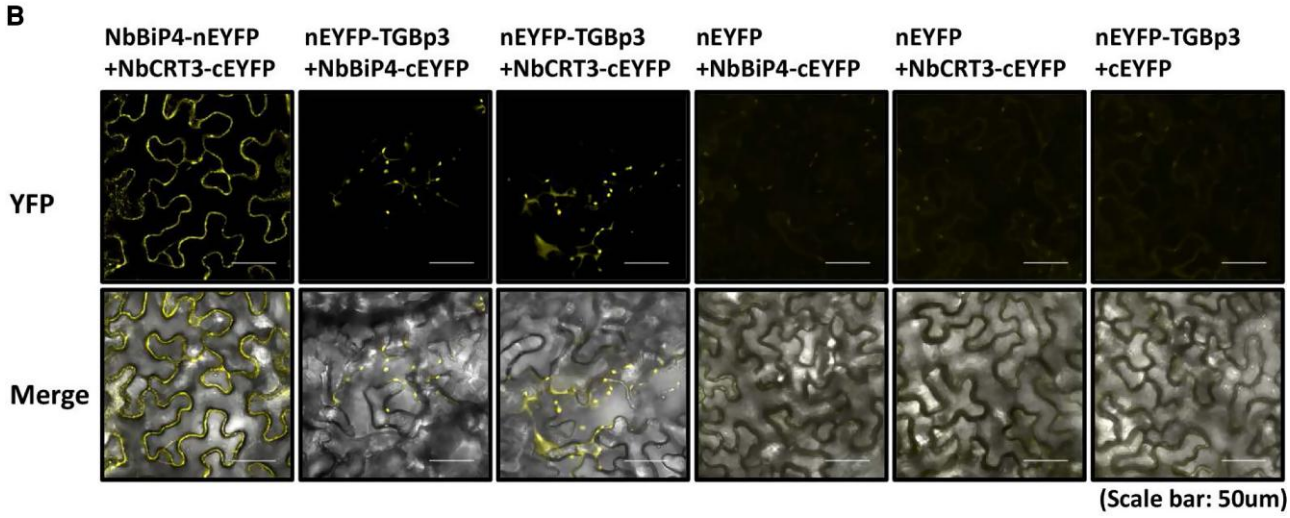

Figure 3 BaMV TGBp3 interacts with NbBiP4 or NbCRT3. A, Analysis of the interaction between BaMV proteins and NbBiP4 or NbCRT3 in *N. benthamiana* using GFP pull-down assay. The expression clones pEGFP, pENbBiP-GFP, pENbCRT-GFP, and p35S::TGBp2p3-TbID and infectious clone pKBRepHA21 were co-expressed with the combinations indicated above each lane. At 3 dpai, total proteins (input) were isolated for GFP-trap pull-down assays. The input proteins were detected by immunoblotting with the antibodies against GFP and HA (left top and middle panels). CBS served as a loading control. After incubation with GFP-Trap and washing, the bound complexes were eluted by boiling, separated on 12% SDS-PAGE, and analyzed for presence of TGBp3-TbID-3XHA, BaMV-CP, TGBp1, and Replicase-HA with corresponding antibodies by immunoblotting (right panels). B, Analysis of interactions between BaMV TGBp3 and NbBiP4 or NbCRT3 using BiFC assay. Fluorescent micrographs of *N. benthamiana* leaf epidermal cells infiltrated with various combinations of EYFP fusion constructs, as indicated above each panel, were shown. Constructs harboring *N*- or C-terminal EYFP fusions are denoted as nEYFP or cEYFP, respectively. The agroinfiltrated *N. benthamiana* leaves were examined by confocal microscopy for complementation of EYFP fluorescence at 3 days post-inoculation (dpi). Scale bar = 50 μm.

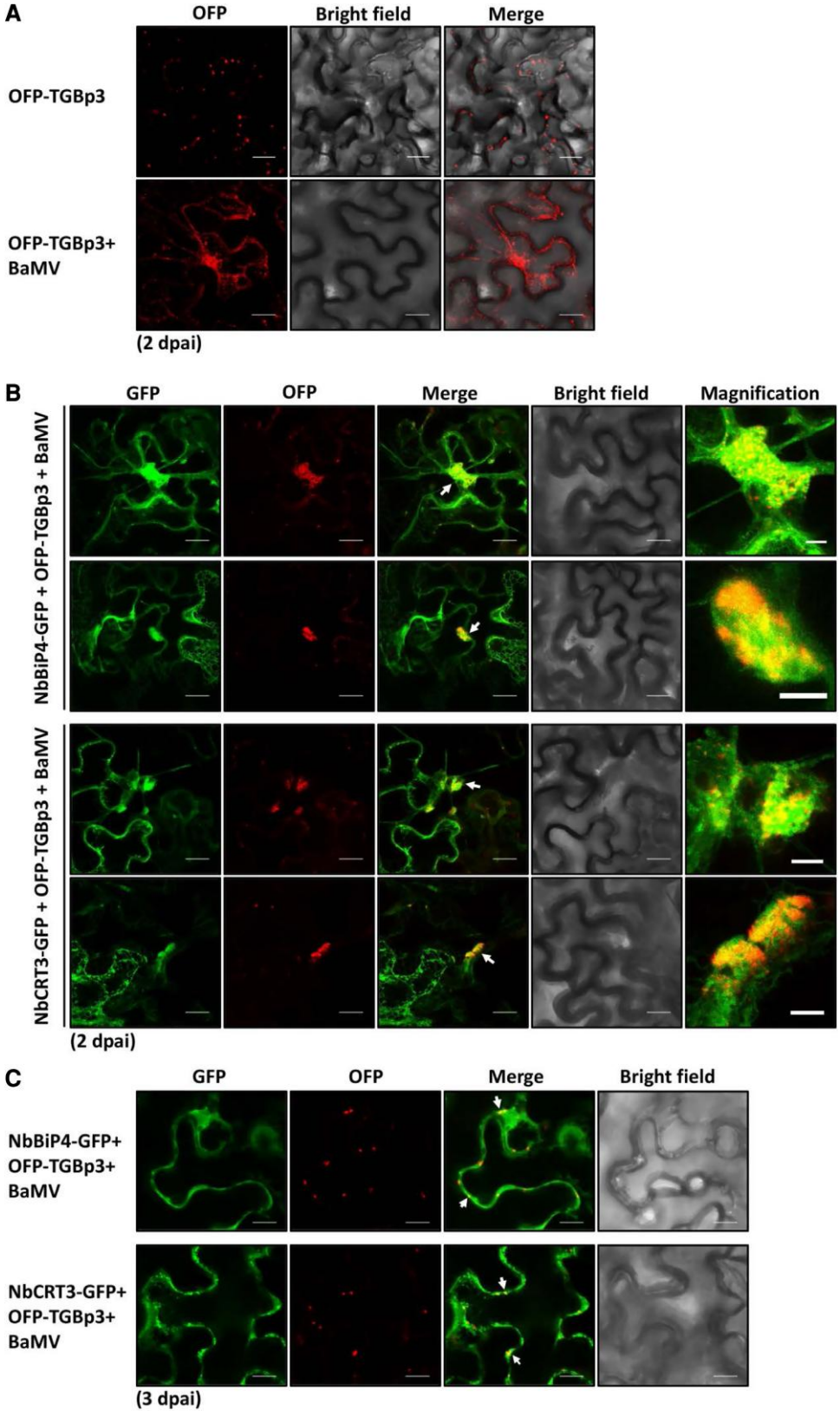

Figure 4 Subcellular localization of OFP-TGBp3 with NbBiP4-GFP or NbCRT3-GFP in BaMV-infected *N. benthamiana*. A, *N. benthamiana* leaf expressing OFP-TGBp3 alone with mock or BaMV infection as indicated. B and C, *A. tumefaciens* harboring p35SOFP-TGBp3 along with pENbBiP-GFP or pENbCRT-GFP was infiltrated into BaMV-infected *N. benthamiana*. Epidermal cells from infiltrated leaves were observed by confocal microscopy with Z-stack at 2 dpai (B) and 3 dpai (C). Scale bar = 20 μm. Scale bars of magnified versions represent 5 μm. White arrows indicate the colocalization of OFP-TGBp3 and NbBiP4-GFP/NbCRT3-GFP.

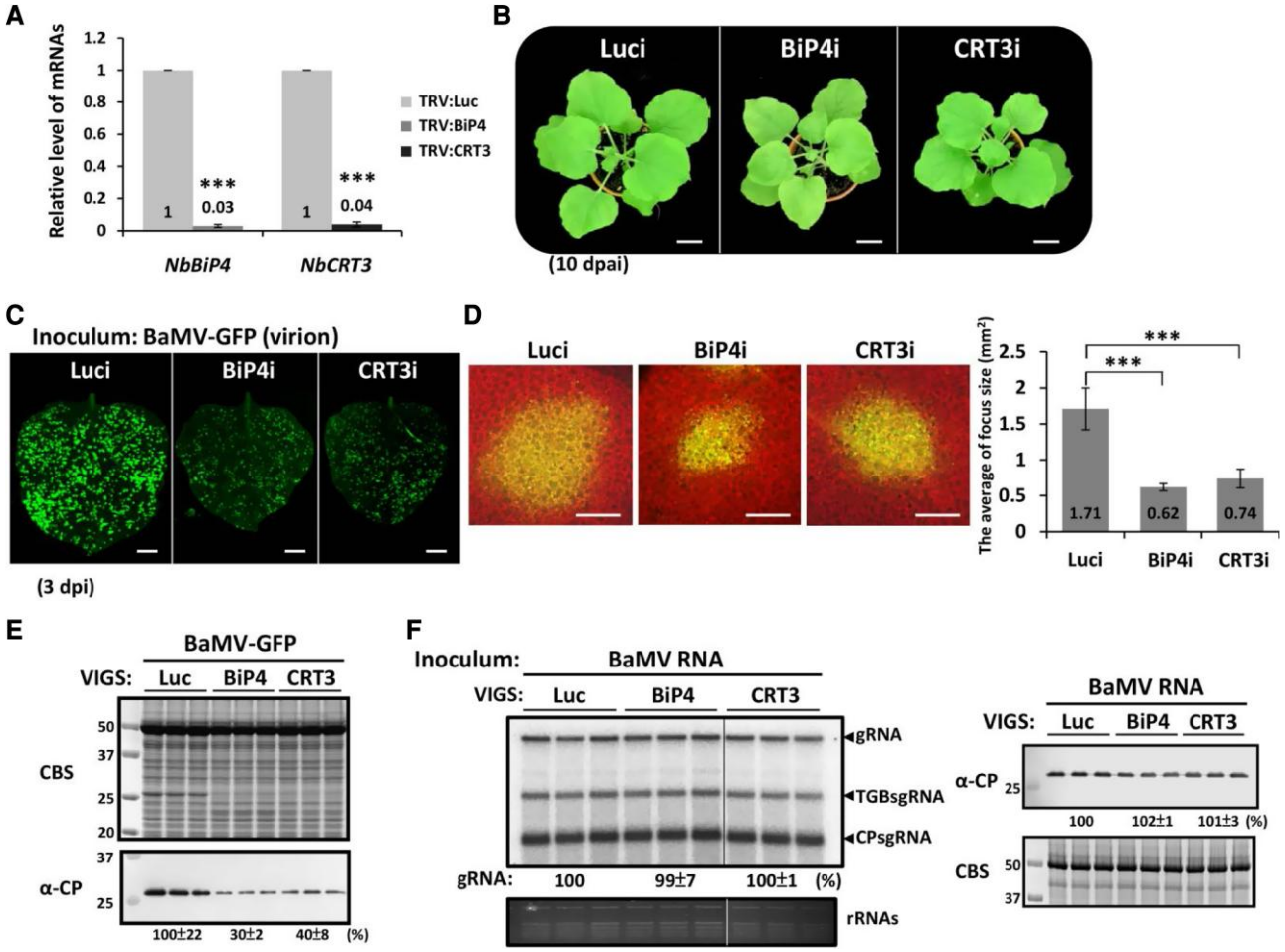

Figure 5 Effect of *NbBiP4* or *NbCRT3* silencing on BaMV accumulation. A, *Tobacco rattle virus* (TRV)-based VIGS was used to silence *NbBiP4* and *NbCRT3*. TRV with *Luciferase* served as VIGS control. The relative expression of *NbBiP4* and *NbCRT3* in control (TRV:Luc) and *NbBiP4*-silenced (TRV:BiP4) or *NbCRT3*-silenced (TRV:CRT3) *N. benthamiana* plants was measured by RT-qPCR at 10 dpai. Data are mean ± SD of at least three independent experiments. Asterisks indicate statistically significant differences between the indicated groups by Student's *t* test (***$P < 0.001$). B, The phenotypes of *NbBiP4*-silenced (BiP4i) and *NbCRT3*-silenced (CRT3i) and control (Luci) *N. benthamiana* at 10 dpai. Scale bar = 2.5 cm. C, Appearance of green fluorescent foci on leaves of the silenced plants infected with BaMV-GFP virion after 3 days post-inoculation (dpi). Scale bar = 1.0 cm. D, Areas of green fluorescent foci were measured by fluorescence microscopy and the results were statistically analyzed for the mean and SD of 20 foci from each plant. Asterisks indicate statistically significant differences of the indicated group by Student's *t* test (***$P < 0.001$). Scale bar = 0.5 mm. E, Western blot analysis of protein levels of BaMV in *N. benthamiana* leaves of (C) for three different plants with antiserum against BaMV-CP. CBS served as a loading control. Data are mean ± SD of BaMV-CP accumulation compared with the control shown below the panel. F, Northern and Western blot analyses of the BaMV RNA and CP accumulation in *Luc-*, *NbBiP4-*, or *NbCRT3*-knockdown protoplasts inoculated with BaMV vRNA at 24 h post-infection. The data shown below the panels are mean accumulation levels of BaMV gRNA or CP when compared with the control.

was downregulated to <10% of that in control plants (Figure 5A), which resulted in a slight growth interference in the plant (Figure 5B). To examine the specificity of RNA silencing, we checked the gene expression of other gene family members of *NbBiP4* and *NbCRT3* by RT-qPCR with gene-specific primers (Supplemental Table 2) at 10 dpi. Silencing of *NbBiP4* did not significantly affect the expression of the other three *NbBiP* homologs (Supplemental Figure 3A). Similarly, knocking down *NbCRT3* did not show off-target effect; instead, *NbCRT3* silencing increased mRNA levels of other two homologs by about two-fold compared with control-silenced plants (Supplemental Figure 3B). The results showed that gene silencing was specific to *NbBiP4* or *NbCRT3* when infiltrated with the corresponding silencing constructs. After confirming the silencing efficiency, the virion of BaMV-GFP was inoculated onto the upper leaves of *NbBiP4-* or *NbCRT3*-silenced plants. BaMV-GFP is a chimeric virus with GFP expression from a duplicated CP subgenomic promoter (Lin et al., 2004), which allows us to observe the BaMV-GFP spreading areas in infected leaf via fluorescence imaging. At 3 days post-inoculation (dpi), much smaller fluorescence foci appeared on the *NbBiP4-* or *NbCRT3*-silenced leaves than the control (Figure 5C). The mean fluorescence area in *Luc-*, *NbBiP4-*, and *NbCRT3*-knockdown plants was

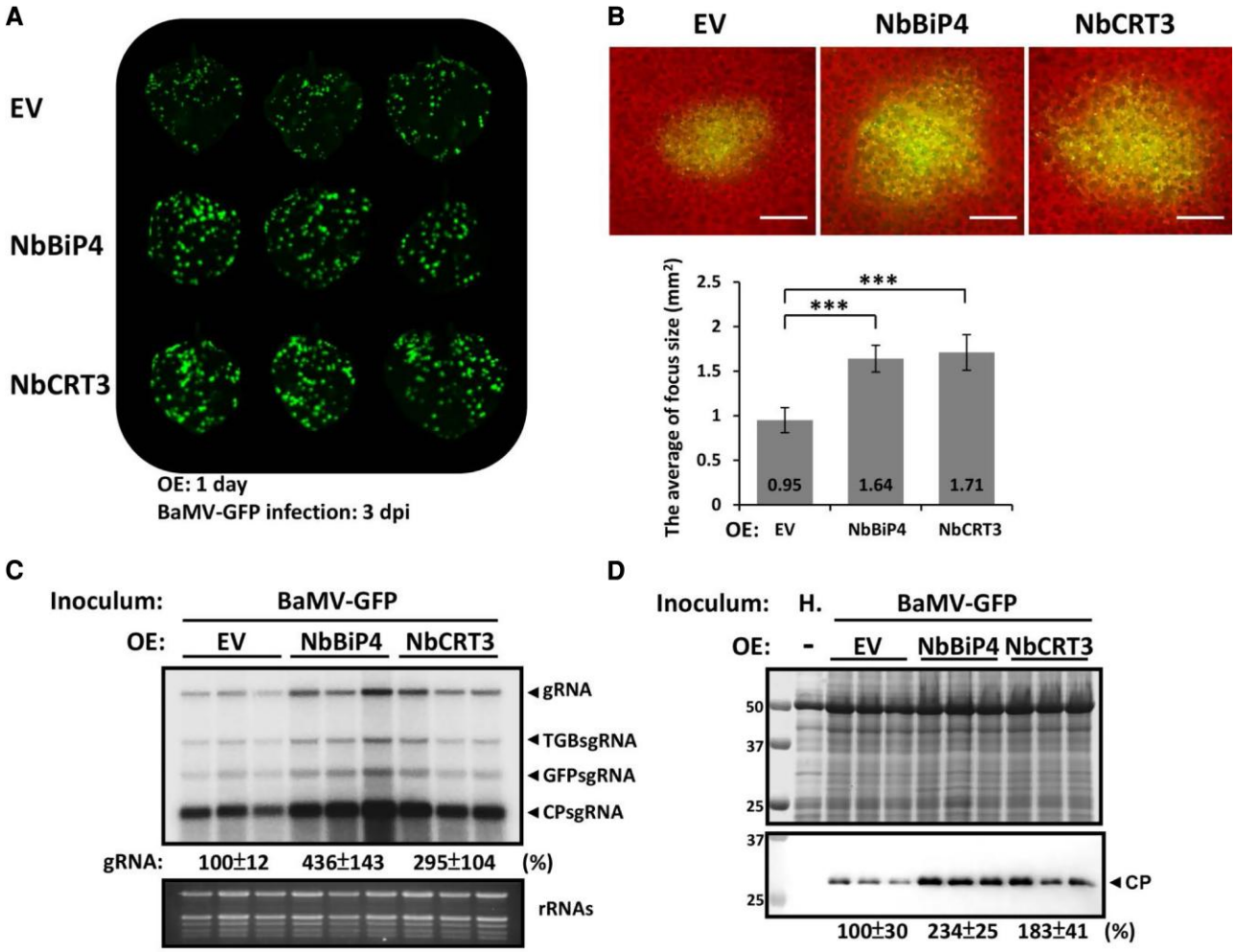

Figure 6 Cell-to-cell movement of BaMV in transiently overexpressed NbBiP4 or NbCRT3 plants. A, Green fluorescence foci on leaves infected with BaMV-GFP. *N. benthamiana* leaves were transiently overexpressed (OE) with empty vector (EV), NbBiP4, or NbCRT3 by *Agrobacterium*-mediated expression for 1 day followed by BaMV-GFP inoculation. The photographs were taken at 3 dpi. B, Areas of green fluorescence foci were measured by fluorescence microscopy and the results were statistically analyzed as the mean and SD of 26 foci from each plant. Scale bar = 0.5 mm. Asterisks indicate statistically significant differences of the indicated group by Student's *t* test (***$P < 0.001$). C and D, Northern (C) and Western (D) blot analyses of BaMV levels in *N. benthamiana* leaves probed with ^{32}P-labeled RNA (C) and antiserum against BaMV-CP (D) for detecting BaMV RNAs and CP, respectively. Data are mean BaMV gRNA or BaMV-CP accumulation compared with the control shown below the panel.

1.71 ± 0.29, 0.62 ± 0.05, and 0.74 ± 0.13 mm^2, respectively (Figure 5D). These results indicated that reducing the expression of *NbBiP4* or *NbCRT3* in *N. benthamiana* made them more resistant to BaMV infection, with less and smaller infection foci than in control plants. Immunoblot assay revealed that BaMV-CP levels were decreased in *NbBiP4*- and *NbCRT3*-knockdown plants to 30% and 40% of that of control plants, respectively, which suggests that NbBiP4 and NbCRT3 enhance the accumulation of BaMV (Figure 5E).

To determine whether reduced BaMV-CP accumulation in *NbBiP4*- or *NbCRT3*-knockdown plants was due to suppressed viral RNA replication, we prepared protoplasts from *NbBiP4* or *NbCRT3*-knockdown plants and transfected with BaMV viral RNA. The RNA and protein accumulations of BaMV in protoplasts from *NbBiP4*- and *NbCRT3*-knockdown and control plants did not show substantial difference (Figure 5F). These results indicate that knockdown of *NbBiP4* or *NbCRT3* expression does not influence BaMV replication at the single-cell level. Thus, NbBiP4 and NbCRT3 should be involved in regulating BaMV cell-to-cell movement.

To test the specificity of the effect of *NbBiP4* or *NbCRT3* expression on different viruses, we inoculated protoplasts prepared from *NbBiP4* or *NbCRT3*-knockdown plants with PVX, *Tobacco mosaic virus* (TMV), or *Cucumber mosaic virus* (CMV) RNA. It was observed that *NbBiP4*-knockdown decreased PVX-CP accumulation to 62%, but did not substantially affect TMV or CMV-CP accumulation. In contrast, *NbCRT3*-knockdown resulted in similar CP accumulations of PVX, TMV, or CMV as those in control cells (Supplemental Figure 4, left panels). These results indicate that NbBiP4 positively regulates PVX RNA accumulation in single cells. When the virus particles were inoculated in *NbBiP4* or *NbCRT3*-knockdown plants to

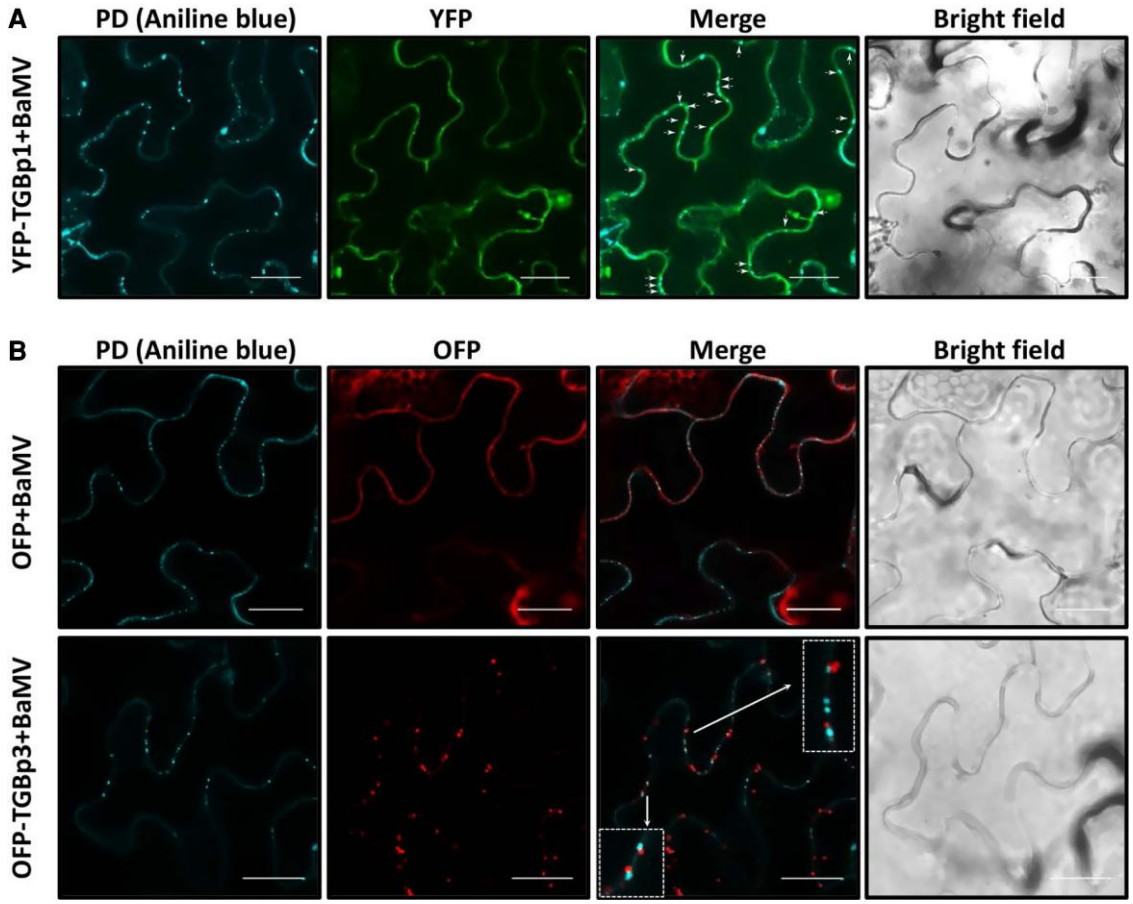

Figure 7 Subcellular localization of BaMV TGBp1/TGBp3 in BaMV-infected *N. benthamiana*. A, PD localization of YFP-TGBp1. *N. benthamiana* leaves were infiltrated by *Agrobacterium* harboring pBAYFP-TGBp1 (YFP-TGBp1) and pKB for 3 dpai. Aniline blue was introduced into the leaves by vacuum infiltration to locate callose in PD. The colocalization of YFP-TGBp1 and PD is indicated by white arrows. Scale bar = 30 μm. B, Subcellular localization of OFP-TGBp3. *N. benthamiana* leaves were infiltrated by *Agrobacterium* harboring p35SOFP (OFP) and pKB (infectious BaMV cDNA clone) or p35SOFP-TGBp3 (OFP-TGBp3) and pKB. Arrows indicate the enlarged images in the white dotted boxes. Scale bar = 30 μm.

further examine their effects on viral infection and spreading, PVX-CP accumulation was reduced to 69% of that in control plants at 3 dpi (Supplemental Figure 4A, right panel). *NbCRT3*-knockdown impaired TMV accumulation, whereas neither *NbBiP4*- nor *NbCRT3*-knowndown affected CMV accumulation (Supplemental Figure 4, B and C, right panels). Altogether, these results indicate that NbBiP4 or NbCRT3 may play different roles at various infection stages in regulating the movement of different viruses, even for those in the same genus. These observations demonstrated the specificity of NbBiP4 and NbCRT3 in facilitating the movement of specific viruses, and provided evidence in support of the notion that the effect of NbBiP4 and NbCRT3 on viral movement is not simply the general chaperone-related functions in ER for all proteins.

Overexpression of NbBiP4 or NbCRT3 enhances cell-to-cell movement of BaMV

Virus infection may induce host gene expression for an environment more favorable to viruses. Since knockdown of *NbBiP4* or *NbCRT3* reduces BaMV infection, we hypothesized that BaMV infection may induce *NbBiP4* and *NbCRT3* to promote virus cell-to-cell movement. To test the hypothesis, the expression levels of *NbBiP4* or *NbCRT3* after BaMV infection were assessed. Total RNAs were extracted from mock- and BaMV-infected *N. benthamiana* leaves at 2, 3, and 5 dpai and analyzed by RT-qPCR. The mRNA level of *NbBiP4* at 2, 3, and 5 dpai was 1.7-, 4.65-, and 7.08-fold higher, respectively, in BaMV-inoculated leaves when compared with those in mock-inoculated leaves (Supplemental Figure 5A), indicating that *NbBiP4* expression is induced during BaMV infection. On the other hand, the mRNA level of *NbCRT3* was 3.8-, 10.5-, and 3.7-fold higher in BaMV-infected leaves than those in control groups at 2, 3, and 5 dpi, respectively (Supplemental Figure 5B). The observation suggested that *NbCRT3* expression is modulated according to different BaMV infection stages.

Since *NbBiP4* and *NbCRT3* are induced during BaMV infection, we transiently overexpressed these proteins to assess their effect on viral infection using BaMV-GFP virions as the reporter in *N. benthamiana*. It was found that much

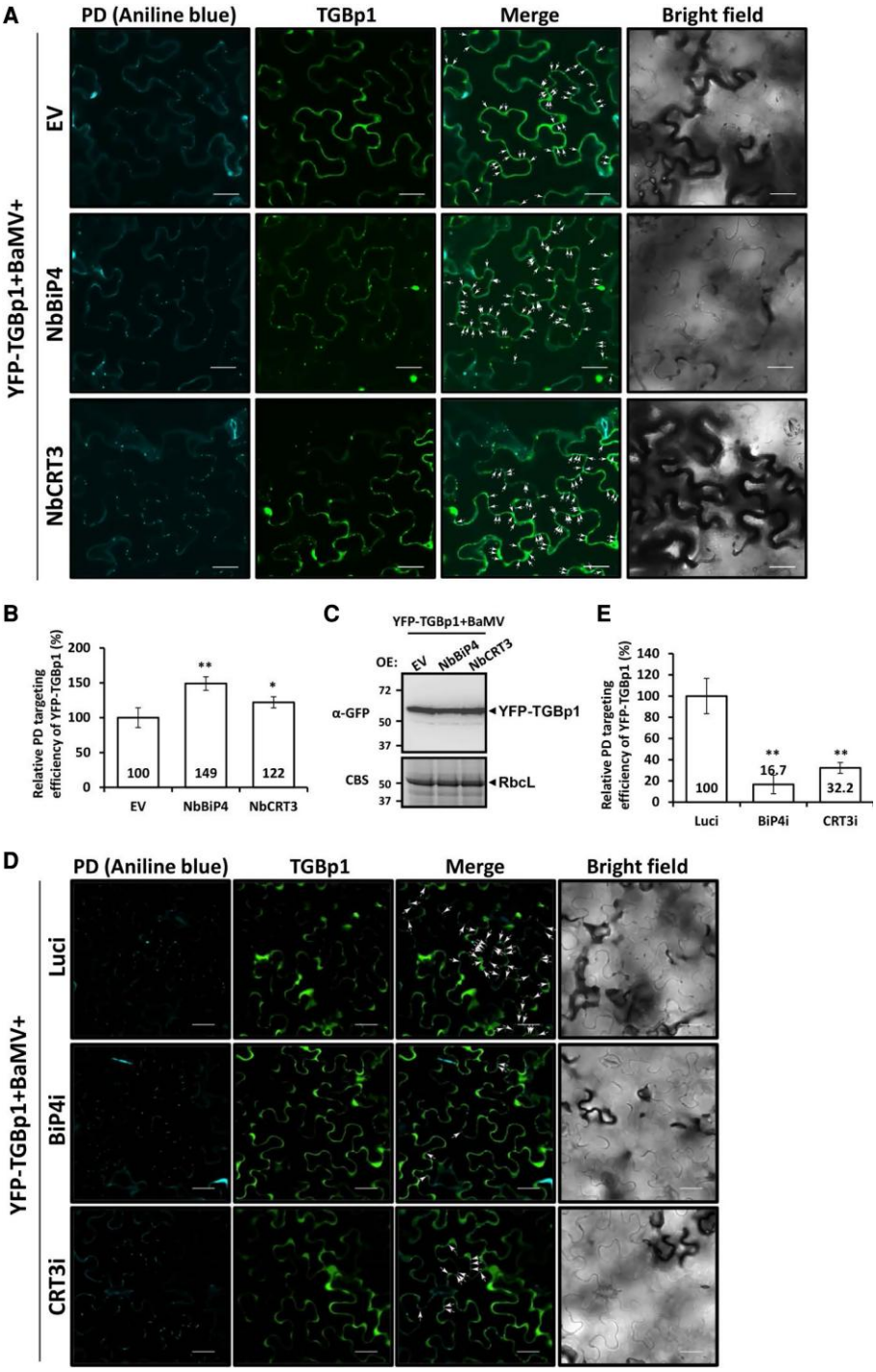

Figure 8 NbBiP4 or NbCRT3 promotes BaMV TGBp1 targeting to PD in *N. benthamiana*. A, PD localization of YFP-TGBp1 in BaMV-infected leaves that transiently overexpressed empty vector (EV), NbBiP4, or NbCRT3 for 3 dpai. Aniline blue was introduced into leaves to locate callose in PD. Arrows indicate the colocalization of YFP-TGBp1 and PD. Scale bar = 30 μm. B, The PD-targeting efficiency of YFP-TGBp1. An independent leaf sample was counted for three different foci of YFP-TGBp1 colocalization with PD and normalized to the corresponding number of PD. The experiment was repeated three times with similar results. Data are mean ± SD of at least three independent experiments. Asterisks in the figure indicate significant differences by Student's *t* test (*$P < 0.05$; **$P < 0.01$). C, Western blot analysis of the accumulation of YFP-TGBp1 protein in *N. benthamiana* leaves overexpressing EV, NbBiP4, or NbCRT3 with anti-GFP antiserum. D, PD localization of YFP-TGBp1 in *Luc-*, *NbBiP4-*, or *NbCRT3*-knockdown *N. benthamiana* epidermal cells. *Agrobacterium* harboring pBAYFP-TGBp1 (YFP-TGBp1) and pKB were infiltrated into silenced leaves for 3 dpai. Aniline blue was introduced into leaves to locate callose in PD. Arrows indicate the colocalization of YFP-TGBp1 and PD. Scale bar = 30 μm. E, The PD-targeting efficiency of YFP-TGBp1 in *Luc-*, *NbBiP4-*, or *NbCRT3*-knockdown *N. benthamiana* cells. Data are mean ± SD of at least three independent experiments. Asterisks in the figure indicate significant differences by Student's *t* test (**$P < 0.01$).

larger fluorescent foci appeared on NbBiP4- or NbCRT3-overexpressing leaves than those on control leaves infiltrated with empty vector (EV; Figure 6A). The mean sizes of foci on the NbBiP4- and NbCRT3-overexpressing leaves were ~1.64 and 1.71 mm^2, respectively, whereas that of foci on control leaves was 0.95 mm^2 (Figure 6B). Northern blot analyses showed that the accumulation of BaMV genomic RNA was 4.36- and 2.95-fold greater, respectively, with NbBiP4 and NbCRT3 overexpression than that in control plants (Figure 6C). Furthermore, the accumulation of BaMV-CP with NbBiP4 and NbCRT3 overexpression was enhanced to 2.34- and 1.83-fold, respectively, when compared with that in control samples (Figure 6D). These data demonstrated that the overexpression of NbBiP4 or NbCRT3 enhanced the BaMV spread in infected leaves.

Since BiP is known to associate with CRT (Crofts et al., 1998; Figure 3B), we reasoned that NbBiP4 and NbCRT3 could play a synergistic role in BaMV cell-to-cell movement. Thus, we co-expressed NbBiP4 and NbCRT3 in *N. benthamiana*, then inoculated the plants with BaMV-GFP. We observed increased mean fluorescence foci size to 1.3- to 1.5-fold when compared with those on leaves expressing NbBiP4 or NbCRT3 alone (Supplemental Figure 6). These results suggested that the interaction or cooperation of NbBiP4 and NbCRT3 may have a greater effect on the cell-to-cell movement of BaMV.

NbBiP4 and NbCRT3 promotes PD targeting of BaMV TGBp1

The above data indicated that NbBiP4 and NbCRT3 may associate with the entire BaMV movement complexes via interaction with TGBp3 and move together along the ER network (Figure 3 and Supplemental Movies 1, A–D). NbBiP4 and NbCRT3 may help the intracellular movement of BaMV to target to cortical ER that forms the tubule structures in PD. Therefore, we investigated the PD localization of TGBp3 and TGBp1 in *N. benthamiana* with florescence-tagged proteins. Because PD localization of TGBp1 requires both TGBp2 and TGBp3 (Chou et al., 2013; Ho et al., 2017), OFP-TGBp3 or yellow fluorescent protein (YFP)-tagged TGBp1 (YFP-TGBp1) was individually co-infiltrated with BaMV. At 3 dpai, YFP-TGBp1 was observed to colocalize with PD as demonstrated by aniline blue staining (Figure 7A), whereas OFP-TGBp3 was not detected in the PD but present in close proximity to PD (Figure 7B). These data suggested that TGBp3 may guide movement complexes in close proximity to PD and help TGBp1 to PD.

Next, we asked if NbBiP4 or NbCRT3 overexpression promotes PD targeting of TGBp1 during BaMV infection. For this NbBiP4, NbCRT3 or EV along with YFP-TGBp1 were introduced into *N. benthamiana* leaves by agroinfiltration, and the leaves were examined at 2 dpai for the fluorescence of YFP-TGBp1 and aniline blue in PD. PD targeting of TGBp1 was enhanced in leaves overexpressing NbBiP4 or NbCRT3 compared with that in the control leaves (Figure 8A). The number of TGBp1 spots localized to PD was counted and normalized to the total aniline blue-stained PD in the corresponding region of interest. The result indicated that overexpression of NbBiP4 or NbCRT3 increased TGBp1 localization to PD by 1.4- and 1.2-fold compared with those in control leaves, respectively (Figure 8B). Immunoblot assay showed a similar accumulation of YFP-TGBp1 in leaves of NbBiP4- or NbCRT3-overexpressing and control groups, which rules out the possibility that enhancing PD targeting was caused by the higher accumulation of YFP-TGBp1 in NbBiP4- or NbCRT3-overexpressing leaves (Figure 8C). To support the conclusion that NbBiP4 or NbCRT3 assists PD targeting of BaMV TGBp1, PD localization of BaMV TGBp1 was examined in *NbBiP4*—or *NbCRT3*—knockdown cells. It was observed that there are very few colocalizations of PD and BaMV TGBp1 in the *NbBiP4*- or *NbCRT3*-silenced cells, when compared with those in the control group (Figure 8D). PD-targeting efficiency of BaMV TGBp1 in *NbBiP4*- and *NbCRT3*-knock downed cells was dramatically reduced to 16.7% and 32.2% of that in control cells, respectively (Figure 8E). Taken together, these data indicated that NbBiP4 and NbCRT3 are necessary for efficient PD localization of TGBp1, which facilitates the movement of BaMV across cells.

Discussion

Cell-to-cell movement of viruses is important for successful infection and plant viruses may co-opt host factors and cellular machinery to fulfill the required functions for movement (Hong and Ju, 2017; Navarro et al., 2019; Kumar and Dasgupta, 2021), due to the limited coding capacity of the small genome sizes of plant viruses. Since PD consists of the cellular membrane, tubules, and cytoskeleton systems, including the plasma membrane, ER, and microtubules, etc., it is expected that some of the host proteins associated with the endomembrane systems, microfilament and microtubule networks, and secretory machineries are involved in the intra- and intercellular movement of various viruses. Ishikawa and colleagues (2017) have demonstrated that the signal peptide-guided targeting of MP of *Fig mosaic virus*, a member of the genus *Emaravirus*, to the microdomains of both ER and plasma membrane is crucial for PD localization. The regulator of synaptic vesicle exo/endocytosis, SYT1, has been shown to directly bind to the MPs of TMV and a geminivirus, Cabbage leaf curl virus, and regulate the recycling of endosomes and MP-mediated cell-to-cell movement through PD (Lewis and Lazarowitz, 2010). Similarly, CRT of different plants have been shown to be involved in the infection process or movement of various viruses, including TMV (Chen et al., 2005), CMV (Choi et al., 2016), PVX (Aguilar et al., 2019), and *Papaya ringspot virus* (Shen et al., 2010). The involvement of components of cytoskeleton systems, ER, and secretion pathways in virus movement has also been well documented. For example, the microtubule-associated protein, MPB2C (MP30 interacting protein), of *Nicotiana tabacum* has been found to

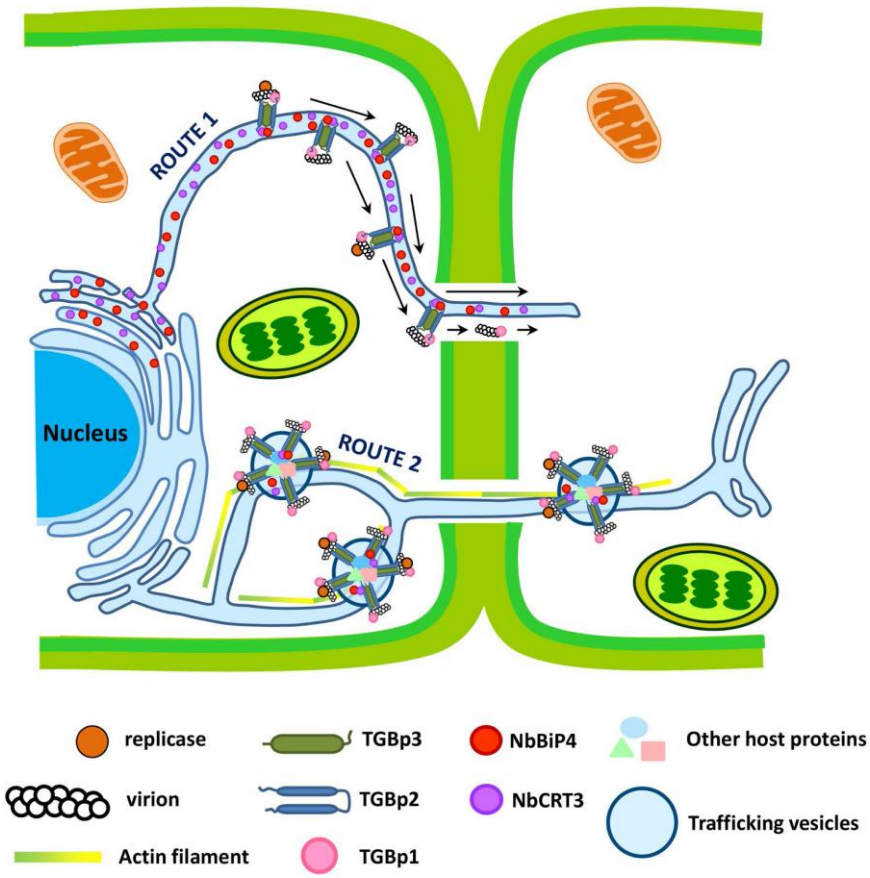

Figure 9 Hypothetical model illustrating how NbBiP4 and NbCRT3 promote intracellular trafficking of BaMV movement complexes. From previous reports (Chou et al., 2013; Liou et al., 2015), two routes are proposed for the intracellular movement of BaMV. Initially, the synthesis of TGB proteins occurs in the perinuclear ER-derived membrane-bound body. The bound complexes of TGBp2 and TGBp3 integrate in the ER membrane and recruit TGBp1, which binds with virion or VRCs that form the BaMV movement complexes. In Route 1, the movement complexes transport along the ER network toward PD via the TGBp3 sorting signals. Alternatively, in Route 2, the movement complexes are combined with a TGBp2-containing vesicle to move along the actin filament to PD. Either in Route 1 or in Route 2, the ER luminal proteins NbBiP4 and NbCRT3 help the BaMV movement complexes toward cortical ER and PD, followed by increasing the SEL of PD by TGBp1 and passing through cell walls in the form of virion or a VRC for efficient movement from one cell to the next.

bind to the MP of TMV and interfere with the cell-to-cell movement (Kragler et al., 2003). The formation and transport of the 6K2 motile vesicles of two potyviruses, *Tobacco etch virus* and *Turnip mosaic virus* (TuMV) have been shown to require the interaction between 6K2 and host proteins involved in those of the COPI and COPII vesicles of the secretory system (Wei and Wang, 2008; Grangeon et al., 2012). For alphaflexiviruses with TGBp types of MP, many host proteins are known to interact with TGBp1 and TGBp2 in regulation of the cell-to-cell movement, as mentioned above. However, there is still a knowledge gap concerning the host factors involved in the interaction network surrounding TGBp3 of alphaflexiviruses. Specifically, the nature of host factors interacting directly or indirectly with TGBp3 of BaMV and other potexviruses remains largely unknown.

Here we used TurboID-based PL approach to tag host factors in close proximity to TGBp3 of BaMV, and identified two ER luminal proteins, NbBiP4 and NbCRT3, that participate in BaMV cell-to-cell movement. Knockdown of *NbBiP4* or *NbCRT3* expression resulted in the formation of smaller infection foci in BaMV-infected leaves when compared with those in the control groups, whereas the replication of BaMV in protoplasts was not substantially affected (Figure 5). These findings indicated that NbBiP4 and NbCRT3 play a role in cell-to-cell spread of BaMV, but not in virus replication process. Confocal microscopy examination revealed that BaMV MP and NbBiP4 or NbCRT3 move together along with the ER network (Supplemental Movie 1). Silencing of *NbBiP4* or *NbCRT3* did not affect the mobility of TGBp3 (Supplemental Movies 2A–2C) but significantly influenced the PD targeting of BaMV movement complex (Figure 8E). Moreover, the overexpression of NbBiP4 or NbCRT3 enhanced PD targeting of BaMV TGBp1 (Figure 8A). Together, our findings indicate that NbBiP4 and NbCRT3 play an important role in the intracellular transport of BaMV.

Although BiP and CRT are well-known chaperone proteins localized in ER lumen that are responsible for co-

and post-translational protein folding and quality control (Kleizen and Braakman, 2004), several lines of evidence suggested that the involvement of NbBiP4 and NbCRT3 proteins in BaMV movement is a unique function exploited by BaMV, and not simply the chaperone-related activities general to all proteins. Firstly, NbBiP4 and NbCRT3 were only labeled by with BaMV TGBp3-TbID with proper movement function, but not by the mutant TGBp3M-TbID that does not possess the correct sorting signal for cortical ER transport nor associate with TGBp1 (Figure 1D and Supplemental Table 1). Secondly, inhibition of NbBiP4 or NbCRT3 expression affected only the size of the infection foci on BaMV-infected leaves, but did not exert substantial effect on BaMV replication in protoplasts (Figure 5). Thirdly, NbBiP4 or NbCRT3 exhibited specificity in facilitating the movement of viruses, affecting the spreading and accumulation of BaMV and PVX, with little or no effect on those of other viruses, such as TMV and CMV, whereas silencing of *NbCRT3* only affected the accumulation of BaMV, PVX, and TMV, but not CMV, in plants (Supplemental Figure 4). In addition, the results of fluorescence microscopy examination revealed the colocalization and co-migration of NbBiP4 or NbCRT3 and the BaMV TGBp3 and movement complexes (Figure 4 and Supplemental Movies 1, A–D). Together, these observations supported that the ability of NbBiP4 and NbCRT3 in facilitating the intracellular movement of BaMV is a unique function exploited by specific viruses, and not just the general chaperone-related activities affecting all proteins.

The increase in expression levels of ER-related chaperon proteins, including BiP (Whitham et al., 2003; García-Marcos et al., 2009; Ye et al., 2011), CRT (Chen et al., 2005), heat shock proteins (HSP70 and HSP90) (Aparicio et al. 2005; Verchot, 2012), in response to ER stress induced by different plant viruses have also been well documented (Herath et al., 2020b). It has been reported that TGBp3 of PVX may induce ER stress and trigger the unfolded protein response, leading to programmed cell death (Ye et al., 2013). The TGBp3 of *Plantago asiatica mosaic virus* (PlAMV, a potexvirus) and the 6K2 protein of TuMV (a potyvirus) are also shown to elicit alternative transcription pathways involving different sets of transcription factors under the ER stress caused by virus infection in Arabidopsis (*Arabidopsis thaliana*; Gayral et al., 2020). It was shown that the activation of transcription factors involved in different ER-to-nucleus stress signaling pathways may result in the specific reduction or enhancement of PlAMV or TuMV. The authors also demonstrated that increasing the protein folding capacity under virus-induced ER stress significantly decreased the accumulation of PlAMV, suggesting that the maintenance of protein folding function is crucial for the plant resistance against virus (Gayral et al., 2020). In contrast, it was found in this study that overexpression of NbBiP4 or NbCRT3 resulted in the promotion of BaMV accumulation (Figure 6). The reasons for the differences in the effects on virus accumulation might be that BaMV TGBp3 may not elicit substantial ER stress in *N. benthamiana*. We have not observed necrotic spots on *N. benthamiana* plants overexpressing BaMV TGBp3 (Supplemental Figure 7) or infected by BaMV, although we have not comprehensively examined the markers for ER stress in these plants, other than the expression of *NbBiP4* and *NbCRT3*. It is also possible that BaMV infection or BaMV TGBp3 could elicit ER stress and trigger the UPR, thereby increasing the expression levels of *NbBiP4* and *NbCRT3* genes (Supplemental Figures 5 and 7C). However, BaMV may exploit the protein chaperone functions of NbBiP4 or NbCRT3 to refold the protein components in the PD channels, the viral RNP complexes, or the VRCs, thereby increasing the SEL of PD or decreasing the sizes of viral RNP or VRC to promote the intercellular movement and enhance BaMV accumulation. Thus, the results in this study might reveal an alternative mode of interaction in which potexviral TGBp3 might recruit the ER-residing chaperones to the site of intercellular movement and exploit the protein refolding function to facilitate viral movement.

There has been evidence that BiP or CRT can associate with viral MPs. BL1 MP of a geminivirus, *squash leaf curl virus* (SqLCV), has been shown to colocalize with BiP in *N. benthamiana* protoplasts (Lazarowitz and Beachy, 1999). However, whether BL1 directly interacts with BiP and the genetic role for BiP in SqLCV movement have not been reported. The MP of TMV was found to directly interact with *N. tabacum* CRT (Chen et al., 2005). In transgenic *N. benthamiana* stably overexpressing maize (*Zea mays*) CRT, TMV accumulation was greatly reduced (Chen et al., 2005). Overexpression of CRT results in mislocalization of TMV MP to microtubules, leading to the interference with the cell-to-cell movement of TMV (Chen et al., 2005). In contrast to TMV, our findings described here show positive regulatory role for NbCRT3 in targeting BaMV TGBp1 MP to PD and BaMV cell-to-cell spread (Figures 6 and 8), NbCRT3 may play a positive regulatory role in BaMV intracellular movement perhaps because it could facilitate the entrance of BaMV TGBp3 into the ER network through interaction, thereby delivering TGBp2- and TGBp3-based movement complexes to PD. Consistent with this, we observed NbCRT3 in the PD, similar to those observed for CRT from maize and *Ar. thaliana* (Baluska et al., 1999; Christensen et al., 2010). Overexpression of NbCRT3 caused large aggregations in the ER lumen in the area of the desmotubule in the PD central cavity (Supplemental Figure 8A) but these aggregates were absent in BaMV-infected samples (Supplemental Figure 8B), suggesting that BaMV can counteract stress induced aggregates in ER lumen.

It should be noted that BaMV TGBp3 has been shown to be a transmembrane protein with the *N*- and C-terminus extending to the ER lumen and cytoplasm, respectively. The observation that the ER lumen localized NbBiP4 and NbCRT3 could be labeled by the TurboID enzyme fused to the C-terminus of BaMV TGBp3 is unexpected. The fact that NbBiP4 and NbCRT3 were only labeled by the functional BaMV TGBp3-TbID, but not by the mutant BaMV TGBp3M-TbID, demonstrated that the identification of

NbBiP4 and NbCRT3 was not an artifact that resulted from the contamination during the purification process, nor the result of co-translational modification. However, the possibility could not be ruled out that NbBiP4 and NbCRT3 might interact and therefore be co-purified with biotinylated TGBp3-TbID by streptavidin beads.

In the TGBp3 interactome, we found BaMV replicase, TGBp1, TGBp2, and CP (Figure 2B). This observation validated our PL approach because our previous study found that all viral proteins are co-purified from TGBp3-containing membrane complexes (Chou et al., 2013). In addition, several host proteins previously identified in the BaMV VRC (Huang et al., 2017a) such as glyceraldehyde 3-phosphate dehydrogenase, HSP70, HSP90, chloroplast phosphoglycerate kinase, eukaryotic elongation factor-1α, and putative methyltransferase and others were also present in the TGBp3 interactome. These findings imply that BaMV movement complexes contain not only the virion but also some pre-virion complex, including double-stranded RNA, replicase, and other components of the replication machinery, that are needed to start the infection cycle again in the neighboring cells. In this scenario, when the complex enters the adjacent uninfected cell, the replication cycle can directly start from the components in the movement complexes that moved in and do not have to start from scratch. Our findings also suggest that the TGBp3-containing membrane complexes may also serve as a base for BaMV virus replication, which is in accordance with the findings of the presence of PVX TGBp3 and replicase in the ER at the same location (Bamunusinghe et al., 2009) with the overlapping functions of replicase in viral movement and replication, and the colocalization of TGBp3-containing granular vesicles with virions in the X-body, where virus replication occurs (Tilsner et al., 2012).

Based on our findings described here combined with the published studies, we propose a hypothetical model for the roles of NbBiP4 and NbCRT3 in intracellular movement of BaMV (Figure 9). Two possible routes for BaMV intracellular movement have been proposed (Chou et al., 2013; Liou et al., 2015). Both routes depend on the TGBp2- and TGBp3-based complex. Route 1 requires the sorting signal of TGBp3 that drives an infectious cargo, TGBp1-virion, to the peripheral ER membrane and in close proximity to PD (Wu et al., 2011; Chou et al., 2013). Mutation of the TGBp3 sorting signal disrupts the ability to assemble with TGBp2 and abolishes delivering the infectious cargo from cell-to-cell (Wu et al., 2011; Figure 1D and Supplemental Table 1B). Subsequently, TGBp1-TGBp2-TGBp3-virion, with or without replicase, forms complexes that move along the ER network toward PD mediated by the targeting signal of TGBp3 and TGBp2 (Wu et al., 2011; Chou et al., 2013; Ho et al., 2017). NbBiP4 and NbCRT3 interact with TGBp3 to help with TGBp3-mediated transportation of BaMV movement complexes (Figure 9, Route 1). In Route 2, TGBp1-virion, or with replicase, associates with TGBp2- and TGBp3-induced vesicles derived from ER membranes to form transportable infectious cargo, which then moves to PD along actin filaments (Hsu et al., 2008; Lee et al., 2010; Liou et al., 2015). In the present study, NbBiP4 or NbCRT3 and TGBp3 were observed in the ER-derived vesicle-like structure and moved together (Figure 4B and Supplemental Movie 1), which might facilitate intra- and intercellular movement of BaMV (Figure 9, Route 2).

In summary, our study revealed an additional function of NbBiP4 and NbCRT3 in the movement of BaMV, and demonstrated that TurboID-based PL is a useful tool for identifying protein complexes or protein–protein interaction networks in virus-infected plants. These findings may pave the way for researchers in developing antiviral strategies for crop protection and further revealing the cellular machineries exploited by viruses during the infection process.

Materials and methods

Viruses and plant materials

BaMV (Accession: AF018156.2), PVX (Accession: AF272736.2), TMV (Ke et al., 2022), and CMV (Hsu et al., 1995) were used for inoculation. *N. benthamiana* plants were grown at 25°C with 16 h light and 8 h dark photoperiod.

Plant inoculation by agroinfiltration

The binary plasmids pKn (empty vector) and pKB (BaMV infectious clone; Liou et al., 2014) were introduced into *Agrobacterium tumefaciens* strain GV3850 individually by electroporation. *A. tumefaciens* cultures were collected by centrifugation and resuspended in infiltration buffer (10 mM MES [pH 5.5], and 10 mM $MgCl_2$); suspensions were adjusted to $OD_{600} = 0.1$ and infiltrated using a needleless syringe into leaves of each test plant.

Proximity labeling

Details on the construction of plasmids p35S::TGBp3-TbID, p35S::TGBp2p3-TbID, p35S::TGBp3M-TbID, and p35S::TGBp2p3M-TbID are described in Supplemental Method 1. Primers used for the plasmid construction are listed in Supplemental Table 2. For PL, leaves of 30-day-old *N. benthamiana* plants were co-infiltrated with agrobacteria harboring a TurboID construct and pKB. After 2 dpai, buffer containing 200 μM biotin (Sigma, Catalog Number B4501) was infiltrated into the same leaf tissues. The infiltrated leaves were harvested after 8 h incubation and extracted total protein by grinding the sample with extraction buffer (50 mM Tris-HCl [pH 8.0], 10 mM KCl, 10 mM $MgCl_2$, 1 mM EDTA, 20% glycerol [v/v], 2% sodium dodecyl sulfate [SDS; w/v], 10% 2-mercaptoethanol [v/v]). Total proteins were separated on 4%–20% gradient or 12% polyacrylamide gels (v/v) containing 1% SDS (w/v) (SDS-PAGE). Separated proteins were stained with Coomassie blue or detected by Western blot analysis with specific antibodies. For Western blot analysis, separated proteins were transferred to PVDF membrane (Millipore, USA), which was incubated with

streptavidin-HRP (Abcam, Catalog number ab7403; 1:20,000 dilution) or primary antibodies against HA-tag (Sigma, Catalog number H6908), BaMV TGBp1 (Chang et al., 1997), or BaMV TGBp2 (Chou et al., 2013) at 1:5,000 dilution.

TurboID sample preparation for MS analysis

After PL, leaves were harvested and frozen in liquid nitrogen. 1 g frozen leaf material was ground to a fine powder in a mortar and protein extraction was performed by addition of 1 mL lysis buffer (50 mM Tris-HCl [pH 7.5], 500 mM NaCl, 1 mM EDTA, 1% NP-40 [v/v; CAS number: 9016-45-9)] 0.1% SDS [w/v], 0.5% sodium deoxycholate [w/v], 1 mM DTT, 1% protease inhibitor cocktail [v/v]; Roche, Germany). After vortex mixing, the tubes were immediately centrifuged at 14,000 g for 10 min at 4°C, upper soluble fraction was then run through the Zeba™ Spin Desalting Column (Thermo Fisher Scientific, Catalog number 89892) to remove the excess biotin in lysates. After estimating the protein concentration, ~3 mg protein in desalted lysates were incubated with 50 µL equilibrated streptavidin-coated magnetic beads (Dynabeads™ MyOne™ Streptavidin C1, Invitrogen, Catalog number 65001) on a rotamixer overnight at 4°C to enrich biotinylated proteins. The beads were sequentially washed once with 1 mL lysis buffer, once with wash buffer 1 (2% SDS [v/v]), once with wash buffer 2 (50 mM HEPES [pH 7.5], 500 mM NaCl, 1 mM EDTA, 0.1% deoxycholic acid [w/v], 1% Triton X-100 [v/v]), and once with wash buffer 3 (10 mM Tris-HCl [pH 7.4], 250 mM LiCl, 1 mM EDTA, 0.1% deoxycholic acid [w/v], 1% NP-40 [v/v]). To remove the potential detergent, the beads were washed twice in 50 mM Tris-HCl (pH 7.5). Finally, the beads were resuspended in 100 µL 50 mM Tris-HCl (pH 7.5). Ten percent of the suspension was taken out for Western blot analysis and the rest of the beads were flash-frozen in liquid nitrogen and identified by liquid chromatography-tandem mass spectrometry (LC/MS-MS) using an Applied Biosystems Sciex/TripleTOF® 6600; QSTAR® Elite spectrometer. Two biological replicates (i.e. two separate sets of plants) were subjected to the analysis as described above for protein identification. The raw data were processed by using Mascot v2.6.0 and searched against the UniProt *N. benthamiana* database and BaMV whole-genome data set.

GFP pull-down assay

Details on the construction of plasmids pENbBiP-GFP and pENbCRT-GFP for GFP pull-down assay are described in Supplemental Method 1. After co-expression of combinations for 2 dpai, total proteins were extracted from agroinfiltrated leaves with use of three volumes of binding buffer (20 mM Tris-HCl [pH 7.5], 2 mM $MgCl_2$, 300 mM NaCl, 5 mM DTT, 0.5% NP-40 [v/v]), and 1% protease inhibitor cocktail (v/v). Total proteins were centrifuged at 4,000 g for 10 min at 4°C and the supernatant was transferred to a new tube as the input. To pull-down the GFP-fused protein binding complexes, the input was incubated with GFP-Trap_M beads (ChromoTek) with a rotamixer for 2 h at 4°C. After incubation, the beads were washed three times with washing buffer (20 mM Tris-HCl [pH 7.5], 2 mM $MgCl_2$, 300 mM NaCl, 5 mM DTT, 1.5% NP40 [v/v]). Finally, the complex containing beads was resuspended in sample buffer for Western blot analysis.

Bimolecular fluorescence complementation

Details on the construction of plasmids for BiFC are described in Supplemental Method 1. *A. tumefaciens* cells harboring various constructs were collected by centrifugation and resuspended in infiltration buffer. Pairs of cultures carrying the respective fusion constructs were adjusted to a concentration of 1.0 at OD_{600}, mixed at a 1:1 volume ratio, and co-infiltrated into *N. benthamiana* leaves. Confocal images were obtained by UPLSAPO 60× water immersion objective lenses (Olympus, Japan) from inoculated leaves 3 days after infiltration. Image acquisition was set to 1,024×1,024 pixels with 8.0 (us/pixel) scan speed. For YFP excitation, 515-nm laser line was used with 2% laser power excitation. Confocal images were obtained using the camera system version 2.3.1.163. Images were merged and adjusted by the software FV31S-SW.

Subcellular localization by confocal microscopy

Details on the construction of plasmids p35SGFP-TGBp3 and p35SOFP-TGBp3 for investigating the subcellular localization are described in Supplemental Method 1. The *A. tumefaciens* GV3850 strain harboring the pENbBiP-GFP or pENbCRT-GFP was individually co-infiltrated with p35SOFP-TGBp3 into *N. benthamiana* leaves. Confocal images were obtained by UPLSAPO 100× oil immersion objective lenses (Olympus) from inoculated leaves 2 and 3 days after infiltration. Image acquisition was set to 1,024×1,024 pixels with 8.0 (us/pixel) scan speed. For GFP and OFP excitation, 488- and 543-nm laser line were used with 2% laser power excitation, respectively. Confocal images were obtained using the camera system version 2.3.1.163. Images were merged and adjusted by the software FV31S-SW. To visualize PD in leaf epidermal cells, we infiltrated aniline blue fluorochrome (0.1 mg/mL in water, Biosupplies) into the agroinfiltrated leaves of *N. benthamiana* and analyzed the sample immediately using FV3000. Image was captured by the use of FLUOVIEW software with 405-, 515-, and 543-nm laser excitation for aniline blue fluorochrome, YFP, and OFP, respectively.

Virus-induced gene silencing

TRV-based VIGS was used to knockdown the expression of *NbBiP4* or *NbCRT3* (Ratcliff et al., 2001). Plasmids pTRV1 and pTRV2-Luc were kindly provided by David C. Baulcombe (Department of Plant Sciences, University of Cambridge, UK). Details on the construction of plasmids pTRV2-NbBiP and pTRV2-NbCRT for VIGS are described in Supplemental Method 1. The constructs pTRV1, pTRV2-Luc, pTRV2-NbBiP, and pTRV2-NbCRT were individually transformed into *A. tumefaciens* strain C58C1 for knockdown experiments. *A. tumefaciens* cultures (OD_{600}, 0.5) containing pTRV2-Luc,

pTRV2-NbBiP, or pTRV2-NbCRT was mixed with pTRV1-containing C58C1 at a 1:1 volume ratio and co-infiltrated by syringe onto three leaves of each test plant. At 10 dpai, the third and fourth leaves above the infiltrated leaves were harvested, and subjected to total RNA isolation by using TriPure reagent (Roche Life Science, Germany), according to the manufacturer's instructions. For measuring the mRNA levels of *NbBiP4* or *NbCRT3* homologs, RT-qPCR was used with the gene-specific primers (Supplemental Table 2). There are four *BiP* homologs that were identified in *N. benthamiana* available at the Sol Genomics Network database (Herath et al., 2020a). We used these sequences to query *N. benthamiana* Transcriptomes V6.1 database (Nakasugi et al., 2013) and to find the transcripts. For the *NbCRT* gene family, Arabidopsis *CRT* (*AtCRT*1–3) sequence were used to blast against the SOlGen database (*N. benthamiana* Genome v1.0.1 predicted cDNA; Bombarely et al., 2012). According these sequences, we designed primer sets to specifically amplify *NbBiP4* and *NbCRT3* homologs (Supplemental Table 2). To normalize the mRNA levels of target genes between samples, relative mRNA levels of *actin* were determined with the primers Actin-F (5′-GATGAAGATACTCACAGAAAGA-3′) and Actin-R (5′-GTGGTTTCATGAATGCCAGCA-3′).

At 10 dpai, 200 ng of viral particles of BaMV-GFP (Lin et al., 2004) was mechanically inoculated into the fourth leaf above the infiltrated leaves. Total proteins were extracted from virus-inoculated leaves at 3 dpi. For the detection of BaMV cell-to-cell movement, fluorescence derived from GFP accompanied by BaMV movement was captured by fluorescent microscopy (Olympus IX71) at 3 dpi with an excitation wavelength of 488 nm, an emission wavelength of 510 nm. The area of each lesion was measured using the software Cellsens (Olympus). For the protoplast assays, protoplasts were isolated from the fourth leaf above *N. benthamiana* leaves infiltrated with TRV:Luc, TRV:BiP4, or TRV:CRT3, respectively. For each inoculation, 0.5 μg of viral RNA was used to inoculate 2×10^5 protoplasts as described previously (Cheng and Tsai, 1999). The inoculated protoplasts were incubated at 25°C under constant light. Total RNA was extracted from protoplasts after 24 h of incubation.

Transient expression of NbBiP4 and NbCRT3 in *N. benthamiana*

Details on the construction of plasmids pENbBiP and pENbCRT for overexpressing NbBiP4 and NbCRT3 in *N. benthamiana* are described in Supplemental Method 1. The resulting plasmid was introduced into *A. tumefaciens* strain GV3850 individually by electroporation. *A. tumefaciens* cultures were collected by centrifugation and resuspended in infiltration buffer. Suspensions were adjusted to $OD_{600} = 0.5$ and infiltrated by needleless syringe into leaves of each test plant.

RNA analysis by northern blot hybridization

Total RNA was extracted from infiltrated leaves or inoculated protoplasts with use of TriPure Isolation Reagent (Roche Life Science). RNA samples were separated by electrophoresis after denaturation in the presence of glyoxal and transferred to nylon membranes (Amersham, UK) for Northern blot analysis (Lin et al., 1996). Blots were hybridized with the riboprobe specific for the 3′-UTR of BaMV or PVX. The ^{32}P-labeled probes were individually transcribed from *Hind*III-linearized pBaHB or pPVXHE by using SP6 and T7 RNA polymerase, respectively (Lin et al., 1993; Huang et al., 2012). The signals were obtained and quantified by using the Amersham Typhoon 5 phosphoimager (GE Healthcare).

Protein analysis and antibodies

Total proteins were extracted from infiltrated leaves or inoculated protoplasts and separated on 12% SDS-PAGE (v/v). Separated proteins were stained with Coomassie blue or detected by Western blot analysis with specific antibodies. For Western blot analysis, separated proteins were transferred to polyvinylidene fluoride membrane (Millipore), which was incubated with the laboratory-generated primary antiserum from rabbits against BaMV-CP, PVX-CP, TMV-CP, CMV-CP, or T7-tag at 1:5,000 dilution.

Statistical analysis

All experiments were conducted three times independently with three biological replicates. The data presented are the means and standard deviations (SDs) of three independent experiments. Statistical differences were determined using Student's *t* test. Significant differences are indicated by asterisks (*$P < 0.05$; **$P < 0.01$; ***$P < 0.001$).

Accession numbers

Sequence data from this article can be found in the GenBank data libraries under accession numbers FJ463755.1 (NbBiP4) and LC409060.1 (NbCRT3).

Supplemental data

Supplemental Figure S1. Complementation of TGBp3-defective BaMV in *N. benthamiana* leaves transiently expressing TGBp3 fusions.

Supplemental Figure S2. Colocalization of BaMV TGBp3, NbBiP4, or NbCRT3 with endoplasmic reticulum (ER) in *N. benthamiana*.

Supplemental Figure S3. RT-qPCR analysis of mRNA levels of *BiP* or *CRT* homologs in *NbBiP4*- or *NbCRT3*- knockdown *N. benthamiana* plants.

Supplemental Figure S4. The effect of *NbBiP4* or *NbCRT3* silencing on PVX, TMV, or CMV accumulation in *N. benthamiana* protoplasts and plants.

Supplemental Figure S5. The expression of *NbBiP4* or *NbCRT3* in BaMV-inoculated *N. benthamiana*.

Supplemental Figure S6. Synergistic effect of NbBiP4 and NbCRT3 in promoting the cell-to-cell movement of BaMV.

Supplemental Figure S7. Expression of *NbBiP4* or *NbCRT3* after delivery of BaMV TGBp3 to *N. benthamiana*.

Supplemental Figure S8. Plasmodesmata (PD) localization of NbCRT3-GFP in mock- (−BaMV) or BaMV-infected (+BaMV) leaves.

Supplemental Movie S1. Mobility of TGBp3 with NbBiP4 or NbCRT3 in the epidermal cells of *N. benthamiana*.

Supplemental Movie S2. Mobility of TGBp3 in the control (Luci), *NbBiP4* (Bip4i)- or *NbCRT3* (CRT3i)-knockdown epidermal cells of *N. benthamiana*.

Supplemental Methods S1. Supplementary Methods.

Supplemental Table S1. List of proteins that are proximal to the BaMV TGBp3-TbID/TGBp3M-TbID.

Supplemental Table S2. List of primers used in this study.

Author contributions

Y.W.H. designed the methodology, performed the experiments, and wrote the original draft; C.I.S. performed the experiments; C.C.H. and Y.H.H. designed the research, interpreted the data, and revised the manuscript; C.H.T., M.M., N.S.L., and S.P.D.K. provided study materials, participated in data discussion, and revised the manuscript.

Acknowledgment

The authors thank the Cell Image Core Laboratory of the Graduate Institute of Biotechnology for providing technical assistance.

Funding

This work was financially supported in part by the Ministry of Science and Technology, Taiwan (MOST-111-2313-B-005-004) and the Advanced Plant Biotechnology Center from The Featured Areas Research Center Program within the framework of the Higher Education Sprout Project by the Ministry of Education (MOE) in Taiwan.

Conflict of interest statement. Authors declare that there is no conflict of interest.

References

Aguilar E, Del Toro FJ, Brosseau C, Moffett P, Canto T, Tenllado F (2019) Cell death triggered by the P25 protein in potato virus X-associated synergisms results from endoplasmic reticulum stress in *Nicotiana benthamiana*. Mol Plant Pathol **20**: 194–210

Angell SM, Davies C, Baulcombe DC (1996) Cell-to-cell movement of potato virus X is associated with a change in the size-exclusion limit of plasmodesmata in trichome cells of *Nicotiana clevelandii*. Virology **216**: 197–201

Aparicio F, Thomas CL, Lederer C, Niu Y, Wang D, Maule AJ (2005) Virus induction of heat shock protein 70 reflects a general response to protein accumulation in the plant cytosol. Plant Physiol **138**: 529–536

Atabekov JG, Rodionova NP, Karpova OV, Kozlovsky SV, Poljakov VY (2000) The movement protein-triggered in situ conversion of potato virus X virion RNA from a nontranslatable into a translatable form. Virology **271**: 259–263

Baluska F, Samaj J, Napier R, Volkmann D (1999) Maize calreticulin localizes preferentially to plasmodesmata in root apex. Plant J **19**: 481–488

Bamunusinghe D, Hemenway CL, Nelson RS, Sanderfoot AA, Ye CM, Silva MAT, Payton M, Verchot-Lubicz J (2009) Analysis of potato virus X replicase and TGBp3 subcellular locations. Virology **393**: 272–285

Bombarely A, Rosli HG, Vrebalov J, Moffett P, Mueller LA, Martin GB (2012) A draft genome sequence of *Nicotiana benthamiana* to enhance molecular plant-microbe biology research. Mol Plant Microbe Interact **25**: 1523–1530

Branon TC, Bosch JA, Sanchez AD, Udeshi ND, Svinkina T, Carr SA, Feldman JL, Perrimon N, Ting AY (2018) Efficient proximity labeling in living cells and organisms with TurboID. Nat Biotechnol **36**: 880–887

Chang CH, Hsu FC, Lee SC, Lo YS, Wang JD, Shaw J, Taliansky M, Chang BY, Hsu YH, Lin NS (2016) The nucleolar fibrillarin protein is required for helper virus-independent long-distance trafficking of a subviral satellite RNA in plants. Plant Cell **28**: 2586–2602

Chang BY, Lin NS, Liou DY, Chen JP, Liou GG, Hsu YH (1997) Subcellular localization of the 28 kDa protein of the triple-gene-block of bamboo mosaic potexvirus. J Gen Virol **78**: 1175–1179

Chen MH, Tian GW, Gafni Y, Citovsky V (2005) Effects of calreticulin on viral cell-to-cell movement. Plant Physiol **138**: 1866–1876

Cheng CP, Tsai CH (1999) Structural and functional analysis of the 3′ untranslated region of bamboo mosaic potexvirus genomic RNA. J Mol Biol **288**: 555–565

Cheng SF, Tsai MS, Huang CL, Huang YP, Chen IH, Lin NS, Hsu YH, Tsai CH, Cheng CP (2013) Ser/Thr kinase-like protein of *Nicotiana benthamiana* is involved in the cell-to-cell movement of bamboo mosaic virus. PLoS One **8**: e62907

Choi Y, Kang MY, Lee JH, Kang WH, Hwang JN, Kwon JK, Kang BC (2016) Isolation and characterization of pepper genes interacting with the CMV-P1 helicase domain. PLoS One **11**: e0146320

Chou YL, Hung YJ, Tseng YH, Hsu HT, Yang JY, Wung CH, Lin NS, Meng MS, Hsu YH, Chang BY (2013) The stable association of virion with the triple-gene-block protein 3-based complex of bamboo mosaic virus. PLoS Pathog **9**: e1003405

Christensen A, Svensson K, Thelin L, Zhang WJ, Tintor N, Prins D, Funke N, Michalak M, Schulze-Lefert P, Saijo Y, et al. (2010) Higher plant calreticulins have acquired specialized functions in *Arabidopsis*. PLoS One **5**: e11342

Citovsky V, Lee LY, Vyas S, Glick E, Chen MH, Vainstein A, Gafni Y, Gelvin SB, Tzfira T (2006) Subcellular localization of interacting proteins by bimolecular fluorescence complementation in planta. J Mol Biol **362**: 1120–1131

Crofts AJ, Leborgne-Castel N, Pesca M, Vitale A, Denecke J (1998) Bip and calreticulin form an abundant complex that is independent of endoplasmic reticulum stress. Plant Cell **10**: 813–823

DiMaio F, Chen CC, Yu X, Frenz B, Hsu YH, Lin NS, Egelman EH (2015) The molecular basis for flexibility in the flexible filamentous plant viruses. Nat Struct Mol Biol **22**: 642–644

Dorokhov YL, Sheshukova EV, Byalik TE, Komarova TV (2020) Diversity of plant virus movement proteins: what do they have in common? Processess **8**: 1547

Fridborg I, Grainger J, Page A, Coleman M, Findlay K, Angell S (2003) TIP, a novel host factor linking callose degradation with the cell-to-cell movement of potato virus X. Mol Plant-Microbe Interact **16**: 132–140

García-Marcos A, Pacheco R, Martiáñez J, González-Jara P, Díaz-Ruíz JR, Tenllado F (2009) Transcriptional changes and oxidative stress associated with the synergistic interaction between potato virus X and potato virus Y and their relationship with symptom expression. Mol Plant-Microbe Interact **22**: 1431–1444

Gayral M, Gaguancela OA, Vasquez E, Herath V, Flores FJ, Dickman MB, Verchot J (2020) Multiple ER-to-nucleus stress signaling pathways are activated during plantago asiatica mosaic virus and turnip mosaic virus infection in *Arabidopsis thaliana*. Plant J **103**: 1233–1245

Grangeon R, Agbeci M, Chen J, Grondin G, Zheng H, Laliberté JF (2012) Impact on the endoplasmic reticulum and Golgi apparatus of Turnip mosaic virus infection. J Virol **86**: 9255–9265

Herath V, Gayral M, Adhikari N, Miller R, Verchot J (2020a) Genome-wide identification and characterization of *Solanum tuberosum* BiP genes reveals the role of the promoter architecture in BiP gene diversity. Sci Rep **10**: 11327

Herath V, Gayral M, Miller RK, Verchot J (2020b) BIP and the unfolded protein response are important for potyvirus and potexvirus infection. Plant Signal Behav **15**: 1807723

Ho TL, Lee HC, Chou YL, Tseng YH, Huang WC, Wung CH, Lin NS, Hsu YH, Chang BY (2017) The cysteine residues at the C-terminal tail of bamboo mosaic virus triple gene block protein 2 are critical for efficient plasmodesmata localization of protein 1 in the same block. Virology **501**: 47–53

Hong JS, Ju HJ (2017) The plant cellular systems for plant virus movement. Plant Pathol J **33**: 213–228

Howard AR, Heppler ML, Ju HJ, Krishnamurthy K, Payton ME, Verchot-Lubicz J (2004) Potato virus X TGBp1 induces plasmodesmata gating and moves between cells in several host species whereas CP moves only in *N. benthamiana* leaves. Virology **328**: 185–197

Hsu HT, Chou YL, Tseng YH, Lin YH, Lin TM, Lin NS, Hsu YH, Chang BY (2008) Topological properties of the triple gene block protein 2 of bamboo mosaic virus. Virology **379**: 1–9

Hsu HT, Hsu YH, Bi IP, Lin NS, Chang BY (2004) Biological functions of the cytoplasmic TGBp1 inclusions of bamboo mosaic potexvirus. Arch Virol **149**: 1027–1035

Hsu YH, Tsai CH, Lin NS (2018) Editorial: molecular biology of bamboo mosaic virus-A type member of the potexvirus genus. Front Microbiol **9**: 6

Hsu YH, Wu CW, Lin BY, Chen HY, Lee MF, Tsai CH (1995) Complete genomic RNA sequences of cucumber mosaic virus strain NT9 from Taiwan. J Arch Virol **140**: 1841–1847

Hu Y, Li Z, Yuan C, Jin X, Yan L, Zhao X, Zhang Y, Jackson AO, Wang X, Han C, et al. (2015) Phosphorylation of TGB1 by protein kinase CK2 promotes barley stripe mosaic virus movement in monocots and dicots. J Exp Bot **66**: 4733–4747

Huang YP, Chen JS, Hsu YH, Tsai CH (2013) A putative Rab-GTPase activation protein from *Nicotiana benthamiana* is important for bamboo mosaic virus intercellular movement. Virology **447**: 292–299

Huang YP, Chen IH, Tsai CH (2017a) Host factors in the infection cycle of bamboo mosaic virus. Front Microbiol **8**: 437

Huang YW, Hu CC, Liou MR, Chang BY, Tsai CH, Meng M, Lin NS, Hsu YH (2012) Hsp90 interacts specifically with viral RNA and differentially regulates replication initiation of bamboo mosaic virus and associated satellite RNA. PLoS Pathog **8**: e1002726

Huang YW, Hu CC, Tsai CH, Lin NS, Hsu YH (2017b) Chloroplast Hsp70 isoform is required for age-dependent tissue preference of bamboo mosaic virus in mature *Nicotiana benthamiana* leaves. Mol Plant Microbe Interact **30**: 631–645

Huang YW, Hu CC, Tsai CH, Lin NS, Hsu YH (2019) *Nicotiana benthamiana* Argonaute10 plays a pro-viral role in bamboo mosaic virus infection. New Phytol **224**: 804–817

Hung CJ, Huang YW, Liou MR, Lee YC, Lin NS, Meng MH, Tsai CH, Hu CC, Hsu YH (2014) Phosphorylation of coat protein by protein kinase CK2 regulates cell-to-cell movement of bamboo mosaic virus through modulating RNA binding. Mol Plant Microbe Interact **27**: 1211–1225

Ishikawa K, Hashimoto M, Yusa A, Koinuma H, Kitazawa Y, Netsu O, Yamaji Y, Namba S (2017) Dual targeting of a virus movement protein to ER and plasma membrane subdomains is essential for plasmodesmata localization. PLoS Pathog **13**: e1006463-24

Ju HJ, Brown JE, Ye CM, Verchot-Lubicz J (2007) Mutations in the central domain of potato virus X TGBp2 eliminate granular vesicles and virus cell-to-cell trafficking. J Virol **81**: 1899–1911

Ju HJ, Samuels TD, Wang YS, Blancaflor E, Payton M, Mitra R, Krishnamurthy K, Nelson RS, Verchot-Lubicz J (2005) The potato virus X TGBp2 movement protein associates with endoplasmic reticulum-derived vesicles during virus infection. Plant Physiol **138**: 1877–1895

Kalinina NO, Rakitina DV, Solovyev AG, Schiemann J, Morozov SY (2002) RNA Helicase activity of the plant virus movement proteins encoded by the first gene of the triple gene block. Virology **296**: 321–329

Kawakami S, Watanabe Y, Beachy RN (2004) Tobacco mosaic virus infection spreads cell to cell as intact replication complexes. Proc Natl Acad Sci U S A **101**: 6291–6296

Ke YD, Huang YW, Viswanath KK, Hu CC, Yeh CM, Mitsuda N, Lin NS, Hsu YH (2022) NbNAC42 and NbZFP3 transcription factors regulate the virus inducible NbAGO5 promoter in *Nicotiana benthamiana*. Front Plant Sci **13**: 924482

Kleizen B, Braakman I (2004) Protein folding and quality control in the endoplasmic reticulum. Curr Opin Cell Biol **16**: 343–349

Kragler F, Curin M, Trutnyeva K, Gansch A, Waigmann E (2003) MPB2C, a microtubule-associated plant protein binds to and interferes with cell-to-cell transport of tobacco mosaic virus movement protein. Plant Physiol **132**: 1870–1883

Kumar G, Dasgupta I (2021) Variability, functions and interactions of plant virus movement proteins: what do we know so far? Microorganisms **9**: 695

Lan P, Yeh WB, Tsai CW, Lin NS (2010) A unique Glycine-rich motif at the N-terminal region of bamboo mosaic virus coat protein is required for symptom expression. Mol Plant Microbe In **23**: 903–914

Lazarowitz SG, Beachy RN (1999) Viral movement proteins as probes for intracellular and intercellular trafficking in plants. Plant Cell **11**: 535–548

Lee SC, Wu CH, Wang CW (2010) Traffic of a viral movement protein complex to the highly curved tubules of the cortical endoplasmic reticulum. Traffic **11**: 912–930

Lewis JD, Lazarowitz SG (2010) *Arabidopsis synaptotagmin* SYTA regulates endocytosis and virus movement protein cell-to-cell transport. Proc Natl Acad Sci U S A **107**: 2491–2496

Lin MK, Chang BY, Liao JT, Lin NS, Hsu YH (2004) Arg-16 and Arg-21 in the N-terminal region of the triple-gene-block protein 1 of bamboo mosaic virus are essential for virus movement. J Gen Virol **85**: 251–259

Lin NS, Chen CC, Hsu YH (1993) Post-embedding in situ hybridization for localization of viral nucleic acid in ultra-thin sections. J Histochem Cytochem **41**: 1513–1519

Lin NS, Lee YS, Lin BY, Lee CW, Hsu YH (1996) The open Reading frame of bamboo mosaic potexvirus satellite RNA is not essential for its replication and can be replaced with a bacterial gene. Proc Natl Acad Sci U S A **93**: 3138–3142

Lin NS, Lin BY, Lo NW, Hu CC, Chow TY, Hsu YH (1994) Nucleotide sequence of the genomic RNA of bamboo mosaic potexvirus. J Gen Virol **75**: 2513–2518

Liou MR, Hu CC, Chou YL, Chang BY, Lin NS, Hsu YH (2015) Viral elements and host cellular proteins in intercellular movement of bamboo mosaic virus. Curr Opin Virol **12**: 99–108

Liou MR, Huang YW, Hu CC, Lin NS, Hsu YH (2014) A dual gene-silencing vector system for monocot and dicot plants. Plant Biotechnol J **12**: 330–343

Lucas WJ (2006) Plant viral movement proteins: agents for cell-to-cell trafficking of viral genomes. Virology **344**: 169–184

Lucas WJ, Ham LK, Kim JY (2009) Plasmodesmata—bridging the gap between neighboring plant cells. Trends Cell Biol **19**: 495–503

Meng M, Lee CC (2017) Function and structural organization of the replication protein of bamboo mosaic virus. Front Microbiol **8**: 522

Módena NA, Zelada AM, Conte F, Mentaberry A (2008) Phosphorylation of the TGBp1 movement protein of potato virus X by a *Nicotiana tabacum* CK2-like activity. Virus Res **137**: 16–23

Morozov SY, Solovyev AG (2003) Triple gene block: modular design of a multifunctional machine for plant virus movement. J Gen Virol **84**: 1351–1366

Nakasugi K, Crowhurst RN, Bally J, Wood CC, Hellens RP, Waterhouse PM (2013) De novo transcriptome sequence assembly and analysis of RNA silencing genes of *Nicotiana benthamiana*. PLoS One **8**: e59534

Navarro JA, Sanchez-Navarro JA, Pallas V (2019) Key checkpoints in the movement of plant viruses through the host. Adv Virus Res **104**: 1–64

Nelson BK, Cai X, Nebenfuhr A (2007) A multicolored set of in vivo organelle markers for co-localization studies in *Arabidopsis* and other plants. Plant J **51**: 1126–1136

Nelson RS, Citovsky V (2005) Plant viruses. Invaders of cells and pirates of cellular pathways. Plant Physiol **138**: 1809–1814

Perraki A, Binaghi M, Mecchia MA, Gronnier J, German-Retana S, Mongrand S, Bayer E, Zelada AM, Germain V (2014) Stremorin1.3 hampers potato virus X TGBp1 ability to increase plasmodesmata permeability, but does not interfere with its silencing suppressor activity. FEBS Lett **588**: 1699–1705

Pitzalis N, Heinlein M (2018) The roles of membranes and associated cytoskeleton in plant virus replication and cell-to-cell movement. J Exp Bot **69**: 117–132

Ratcliff F, Martin-Hernandez AM, Baulcombe DC (2001) Tobacco rattle virus as a vector for analysis of gene function by silencing. Plant J **25**: 237–245

Reagan BC, Burch-Smith TM (2020) Viruses reveal the secrets of plasmodesmal cell biology. Mol Plant-Microbe Interact **33**: 26–39

Roberts AG, Oparka KJ (2003) Plasmodesmata and the control of symplastic transport. Plant Cell Environ **26**: 103–124

Samuels TD, Ju HJ, Ye CM, Motes CM, Blancaflor EB, Verchot-Lubicz J (2007) Subcellular targeting and interactions among the potato virus X TGB proteins. Virology **367**: 375–389

Semashko MA, González I, Shaw J, Leonova OG, Popenko VI, Taliansky ME, Canto T, Kalinina NO (2012b) The extreme N-terminal domain of a hordeivirus TGB1 movement protein mediates its localization to the nucleolus and interaction with fibrillarin. Biochimie **94**: 1180–1188

Semashko MA, Rakitina DV, González I, Canto T, Kalinina NO, Taliansky ME (2012a) Movement protein of hordeivirus interacts in vitro and in vivo with coilin, a major structural protein of Cajal bodies. Dokl Biochem Biophys **442**: 57–60

Shen W, Yan P, Gao L, Pan X, Wu J, Zhou P (2010) Helper component-proteinase (HC-pro) protein of papaya ringspot virus interacts with papaya calreticulin. Mol Plant Pathol **11**: 335–346

Solovyev AG, Kalinina NO, Morozov SY (2012) Recent advances in research of plant virus movement mediated by triple gene block. Front Plant Sci **3**: 276

Tilsner J, Linnik O, Wright KM, Bell K, Roberts AG, Lacomme C, Cruz SS, Oparka KJ (2012) The TGB1 movement protein of potato virus X reorganizes actin and endomembranes into the X-body, a viral replication factory. Plant Physiol **158**: 1359–1370

Tseng YH, Hsu HT, Chou YL, Hu CC, Lin NS, Hsu YH, Chang BY (2009) The two conserved cysteine residues of the triple gene block protein 2 are critical for both cell-to-cell and systemic movement of bamboo mosaic virus. Mol Plant Microbe Interact **22**: 1379–1388

Ueki S, Citovsky V (2011) To gate, or not to gate: regulatory mechanisms for intercellular protein transport and virus movement in plants. Mol Plant **4**: 782–793

Verchot-Lubicz J, Torrance L, Solovyev AG, Morozov SY, Jackson AO, Gilmer D (2010) Varied movement strategies employed by triple gene block-encoding viruses. Mol Plant Microbe Interact **23**: 1231–1247

Verchot J (2012) Cellular chaperones and folding enzymes are vital contributors to membrane bound replication and movement complexes during plant RNA virus infection. Front Plant Sci **3**: 275

Wang AM (2015) Dissecting the molecular network of virus-plant interactions: the complex roles of host factors. Annu Rev Phytopathol **53**: 45–66

Wei T, Wang A (2008) Biogenesis of cytoplasmic membranous vesicles for plant potyvirus replication occurs at endoplasmic reticulum exit sites in a COPI- and COPII-dependent manner. J Virol **82**: 12252–12264

Whitham SA, Quan S, Chang HS, Cooper B, Estes B, Zhu T, Wang X, Hou YM (2003) Diverse RNA viruses elicit the expression of common sets of genes in susceptible *Arabidopsis thaliana* plants. Plant J **33**: 271–283

Wu CH, Lee SC, Wang CW (2011) Viral protein targeting to the cortical endoplasmic reticulum is required for cell-cell spreading in plants. J Cell Biol **193**: 521–535

Wung CH, Hsu YH, Liou DY, Huang WC, Lin NS, Chang BY (1999) Identification of the RNA-binding sites of the triple gene block protein 1 of bamboo mosaic potexvirus. J Gen Virol **80**: 1119–1126

Yang CC, Liu JS, Lin CP, Lin NS (1997) Nucleotide sequence and phylogenetic analysis of a bamboo mosaic potexvirus isolate from common bamboo (*Bambusa vulgaris* McClure). Bot Bull Acad Sinica **38**: 77–84

Ye CM, Chen SR, Payton M, Dickman MB, Verchot J (2013) TGBp3 triggers the unfolded protein response and SKP1-dependent programmed cell death. Molecular Plant Pathol **14**: 241–255

Ye CM, Dickman MB, Whitham SA, Payton M, Verchot J (2011) The unfolded protein response is triggered by a plant viral movement protein. Plant Physiol **156**: 741–755

Zhang YL, Li YY, Yang XX, Wen ZY, Nagalakshmi U, Dinesh-Kumar SP (2020) TurboID-based proximity labeling for in planta identification of protein-protein interaction networks. J Vis Exp **159**: e60728

Zhang YL, Song GY, Lai NK, Nagalakshmi U, Li YY, Zheng WJ, Huang PJ, Branon TC, Ting AY, Walley JW, et al. (2019) TurboID-based proximity labeling reveals that UBR7 is a regulator of N NLR immune receptor-mediated immunity. Nat Commun **10**: 3252